
Partial Information Decomposition for Data Interpretability and Feature Selection

Charles Westphal

Department of Computer Science
University College London
ucabwes@ucl.ac.uk

Stephen Hailes

Department of Computer Science
University College London
s.hailes@ucl.ac.uk

Mirco Musolesi

Department of Computer Science
University College London
m.musolesi@ucl.ac.uk

Abstract

In this paper, we introduce Partial Information Decomposition of Features (PIDF), a new paradigm for simultaneous data interpretability and feature selection. Contrary to traditional methods that assign a single importance value, our approach is based on three metrics per feature: the mutual information shared with the target variable, the feature's contribution to synergistic information, and the amount of this information that is redundant. In particular, we develop a novel procedure based on these three metrics, which reveals not only how features are correlated with the target but also the additional and overlapping information provided by considering them in combination with other features. We extensively evaluate PIDF using both synthetic and real-world data, demonstrating its potential applications and effectiveness, by considering case studies from genetics and neuroscience.

1 Introduction

Data interpretability and feature selection are key areas of research in machine learning (ML). One way in which researchers quantify the relative significance of a model's input attributes is by assigning each of them a feature importance. Multiple paradigms for deriving feature importance have been developed over the past decades. Some of these, inspired by techniques from economics, are based on *Shapley value-based approaches* [Keinan et al., 2004, Cohen et al., 2007, Apley and Zhu, 2020, Debeer and Strobl, 2020, Catav et al., 2021, Kwon and Zou, 2022, Janssen et al., 2023]; others instead rely on the quantification of the correlation between the model's target and its features [Peng et al., 2005, Brown et al., 2012, Gao et al., 2016, Chen et al., 2018, Schnapp and Sabato, 2021, Covert et al., 2023]. Feature importances can be used to explain the relationships within the underlying data and select features [Covert et al., 2020, Weinberger et al., 2023]. The authors Catav et al. [2021] and Janssen et al. [2023] highlighted inconsistencies in achieving these dual objectives simultaneously. To illustrate this, let us consider the characteristics required of a procedure that aims to both explain the data and select features. In the presence of perfectly correlated features, the procedure should not only assign identical scores, but also indicate their information is redundant. Otherwise, during selection, both may be included in the final set. Meanwhile, if applied to features that are only informative in combination, the procedure should assign them as important and select them, but only if considered in conjunction. Current methods [Covert et al., 2020, Catav et al., 2021, Janssen et al., 2023, Covert et al., 2023, Weinberger et al., 2023] are not able to satisfy these requirements. This is particularly

problematic when these techniques are applied to scientific data [Catav et al., 2021, Janssen et al., 2023].

To address these problems, in this paper, we develop *partial information decomposition of features (PIDF)*. A novel method that simultaneously explains data and selects features, even in the presence of complex interactions. To achieve this PIDF considers the synergy, redundancy, and mutual information per feature. These three quantities can then be visualized for interpretability, as shown in Figure 1¹. PIDF builds upon the theory of partial information decomposition (PID) [Chechik et al., 2001, Williams and Beer, 2010], which characterizes interactions between variables. However, PID focuses on generic sets of random variables, ignoring their individual contributions to synergy and redundancy. This makes it unsuitable for tasks such as attributing feature importances and examining the input data of ML models. Motivated by this, we develop PIDF in the following two steps. First, we introduce the concepts of *feature-wise synergy (FWS)* and *feature-wise redundancy (FWR)*, which describe relationships between features. Second, we leverage these definitions to design PIDF.

To provide a better intuition of the proposed approach, let us consider the following example. Suppose we are trying to predict housing prices in Northern California, using the following per-property data: longitude, latitude, and distance to the coast. Individually, longitude and latitude offer limited insight into housing prices. However, they combine synergistically to provide an exact location — a highly informative feature. In this context, longitude is redundant when compared to coastal proximity. Standard multivariate formulations of information theory, as applied to this example, seek to answer the following question: do longitude, latitude, and coastal proximity collectively provide redundant or synergistic information about housing prices? Existing methods [Chechik et al., 2001, Williams and Beer, 2010, Griffith and Koch, 2014, Bertschinger et al., 2013, Griffith and Ho, 2015] would fail to recognize the synergistic combination, instead suggesting that our features collectively provide redundant information. By considering per-feature synergy and redundancy, PIDF captures detailed feature interactions, which can subsequently be compactly represented for interpretation.

We perform a comprehensive experimental evaluation using several synthetic and scientific datasets. In particular, as case studies, we consider two datasets containing genetic data and brain network data showing that PIDF can be used to gain a deeper understanding of how genes and neurons interact.

2 Related Work

Dataset interpretability. Feature importances have been used to enhance interpretability and select features [Fisher et al., 2019, Covert et al., 2020, Aas et al., 2021]. However, Catav et al. [2021] highlighted that these dual perspectives do not appear universally consistent. This dilemma prompted Catav et al. [2021] to propose axioms for assigning feature importance when the goal was solely to explain the underlying data. Building on these principles, Janssen et al. [2023] further refined Catav’s axioms for interpretability, while also enhancing speed and ensuring unrelated variables do not receive a non-zero importance rating. However, these axioms fail to handle complex redundancies. Suppose there exist three features, two of which are indistinguishable, one is unique, and all three reduce the uncertainty of the target equally. According to both the ‘Invariance under Redundant Information and Symmetry under Duplication’ and ‘Elimination’ axioms presented in Janssen et al. [2023] and Catav et al. [2021] all three variables will be assigned the same importance. We contend that to explain the underlying relationships within data, it is essential to identify when information is redundant and consequently more disposable. We also note that, while these axioms of feature importance do account for higher order interactions, they cannot distinguish when the interactions are synergistic and which features are involved.

Partial information decomposition of features for feature selection. Within the context of feature selection, the most relevant work to ours is that produced by Wollstadt et al. [2023] as they truly develop a framework for the PID of features. Here, they are not using their PID adaptation to describe the relationships within data and select features. Rather, it is used to explain why certain features were chosen over others. Their method is a derivative of that introduced by Brown et al. [2012], in which a feature is selected if augmenting it to the set of those already chosen maximizes the correlation with the target. At each round of selection, they decompose the contributions of each potential feature according to their adaptation of the PID paradigm. Unfortunately, this method is unable to identify

¹The library implementing PIDF will be made available upon publication and an URL will be added here.

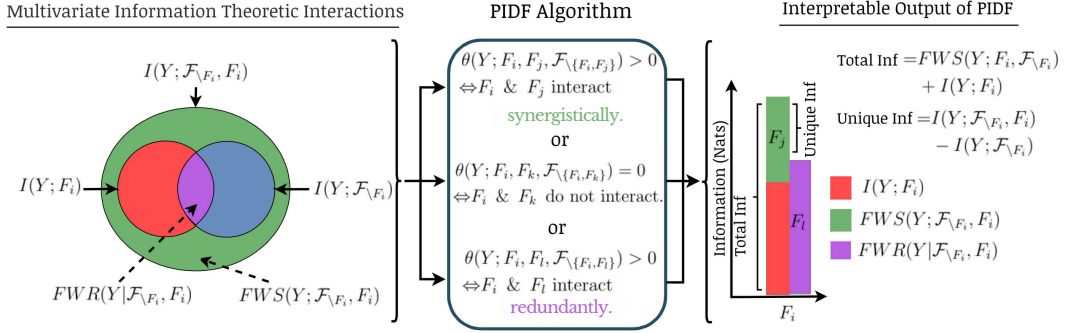


Figure 1: PIDF at a glance. The diagram shows how the information-theoretic interactions (left) between the FOI, FNOI, and target are converted to an interpretable representation by means of a bar graph (right) using PIDF.

fully synergistic variables (i.e., variables that considered alone are non-informative, but combine to describe the target). Such features will not be selected using this method, and their synergy will remain undiscovered. Another feature selection method built upon the theoretical foundations of PID is developed in Westphal et al. [2024]. The authors study how entropy is transferred from the features to the target, sequentially eliminating those with a negligible contribution. This method effectively identifies synergistic variables; however, it does not consistently identify the smaller of two redundant feature subsets. Consider a scenario where a subset of features conveys the same information as a single variable. Unfortunately, the method proposed in Westphal et al. [2024] falls short in consistently choosing the more parsimonious option, which in this case, would be the individual variable.

Open questions. To summarize, it is possible to identify three open questions that the existing solutions fail to tackle, which we aim to address throughout the design and evaluation of PIDF:

The redundant variables question (RVQ): Is it possible to distinguish two fully redundant features from one of their non-redundant counterparts if all three reduce the uncertainty of the target equally?

The synergistic variables question (SVQ): Let us consider the case where two features combine to be fully informative regarding the target, whereas, if taken singularly, they are completely uninformative. Is it possible to reveal these variables are only useful in combination?

The minimal subsets question (MSQ): Suppose there exists multiple perfectly redundant feature subsets, is it possible to consistently select the smallest of these sets?

3 PIDF at a Glance

Let the input to a ML model be denoted $x = (f_1, f_2, \dots, f_N)$, where f_i is a feature instance. By random sampling from the elements of our input list f_i , and from the realizations of the ground truth y , we represent not only all possible features as a set of random variables (written as $\mathcal{F} = \{F_1, F_2 \dots F_N\}$), but also the ground truth (written as Y). Using these distributions, PIDF aims to elucidate *not only the importance of a feature, but also the inter-feature interactions*.

To do this, we aim to develop PIDF, an algorithm that calculates three information-theoretic quantities per feature, FWS, FWR, and MI. These quantities should assist in understanding how the Feature Of Interest (FOI, labelled $F_i \in \mathcal{F}$) interacts with the Features Not Of Interest (FNOIs, labelled $F_j, F_k, F_l \in \mathcal{F}_{\setminus F_i}$), to describe the target.

To enhance the interpretability of PIDFs results, we present these three quantities as shown in Figure 1. Per FOI we will have three bars, the first of which (red), will describe the MI between the FOI and target. The second (green), will quantify the synergistic information provided via the FOI interacting with the FNOI. These red and green bars will stack to give the *total information*. To the right-hand side of this, we will present a purple bar which reveals the extent to which the total information provided by the FOI is redundant. FWS and FWR arise due to interactions; consequently, we label these bars with the FNOI with which these interactions occur. For instance, in Figure 1, we observe that the FOI interacts synergistically with FNOI F_j and redundantly with FNOI F_l .

4 Feature-wise Partial Information Decomposition

Synergy [Anastassiou, 2007], defined as the additional information gained by considering variables jointly, is expressed as: $Syn(Z; X_1, X_2, \dots, X_N) = I(Z; X_1, X_2, \dots, X_N) - \sum_{i=1}^N I(Z; X_i)$. Conditional redundancy [Schneidman et al., 2003] (other definitions are available in Paluř [1996], Williams and Beer [2010], Griffith and Ho [2015]), which refers to the repeated information within variable ensembles, is formulated as: $CR(Z|X_1; X_2; \dots; X_N) = H(Z|X_1, X_2, \dots, X_N) - \sum_{i=1}^N H(Z|X_i)$. In general, these quantities are utilized to describe complete sets of variables [Williams and Beer, 2010]. In the following, for the study of feature importance, we aim to adapt these definitions to understand how the FOI interacts with FNOIs to provide information about the target, i.e., we reformulate both the synergy and redundancy for the purpose of feature interpretability. Although, this does not apply to MI, which remains in its standard form [Shannon, 1948]².

4.1 Measuring Feature-wise Synergy

When assessing the synergistic contribution of an individual feature, the aim is to determine how much extra information the FOI can reveal about the target by combining with the FNOIs. One pre-existing method for doing this is to rewrite the synergy while considering the feature set as a two-body system, where the FOI interacts with the FNOI, such that: $\mathcal{F} = \{F_i, \mathcal{F}_{\setminus F_i}\}$ [Wollstadt et al., 2023]. This leads to the following feature-wise definition of synergy: $Syn(Y; F_i, \mathcal{F}_{\setminus F_i}) = I(Y; F_i, \mathcal{F}_{\setminus F_i}) - I(Y; \mathcal{F}_{\setminus F_i}) - I(Y; F_i)$. However, this definition is not sufficient. To explain why we work through the following simple example: suppose that the FOI (F_i) is completely uninformative in itself, but combines with FNOI $F_j \in \mathcal{F}_{\setminus F_i}$ to fully describe Y (satisfying $I(Y; F_i, F_j) = H(Y)$). Furthermore, let us suppose there also exists another FNOI in our set of features ($F_k \in \mathcal{F}$) which is identical to F_i ($F_i \equiv F_k$). In this case, it is trivial to calculate that $Syn(Y; F_i, \mathcal{F}_{\setminus F_i}) = 0$, due to the information replicated in F_i 's duplicate feature F_k . However, for a full understanding of the underlying data we would like to know that the variable F_i did provide synergistic information about Y in combination with F_j , despite it being redundant. Motivated by this example we define the FWS as the maximum extra information gained by adding the FOI to any subset of $\mathcal{P}(\mathcal{F})$. More formally, this becomes: $FWS(Y; F_i, \mathcal{F}_{\setminus F_i}) = \max_{\mathcal{P}^{ms} \in \mathcal{P}(\mathcal{F}_{\setminus F_i})} Syn(Y; F_i, \mathcal{P}^{ms})$. This describes the extra reduction in uncertainty of the target caused by considering F_i collectively with \mathcal{P}^{ms} , the *subset of maximum synergy*. Combining $FWS(Y; F_i, \mathcal{F}_{\setminus F_i})$ with $I(Y; F_i)$ results in the *total information* ($TI(Y; F_i, \mathcal{F}_{\setminus F_i}) = I(Y; F_i) + FWS(Y; F_i, \mathcal{F}_{\setminus F_i})$), i.e., the maximum possible reduction in uncertainty of the target caused by the FOI. Our goal is to develop an algorithm that reliably derives the subset of maximum synergy, so that $FWS(Y; F_i, \mathcal{F}_{\setminus F_i})$ can appear as the green bar presented in Figure 1.

4.2 Measuring Feature-wise Redundancy

When assessing feature-wise redundancy, our goal is to know how much of the total information ($FWS(Y; F_i, \mathcal{F}_{\setminus F_i}) + I(Y; F_i)$) provided by the FOI is redundant. Consequently, we adopt the following formal definition of FWR: $FWR(Y|F_i, \mathcal{F}_{\setminus F_i}) = CR(Y|F_i, \mathcal{F}_{\setminus F_i}) - \min_{\mathcal{P} \in \mathcal{P}(\mathcal{F}_{\setminus F_i})} (CR(Y|F_i, \mathcal{P}))$. Via the monotonicity of conditional entropy it is trivial to see that $CR(Y|F_i, \mathcal{F}_{\setminus F_i}) = \max_{\mathcal{P} \in \mathcal{P}(\mathcal{F}_{\setminus F_i})} (CR(Y|F_i, \mathcal{P}))$. Therefore, Definition 2 relates the **maximum** and **minimum** possible amounts of redundant information provided by the FOI given all subsets. This is theoretically desirable as the set of minimum redundancy is also the set of maximum synergy (\mathcal{P}^{ms}), meaning FWR can be related to FWS and MI via the following theorem.

Theorem 1: *The difference between the total information (i.e., $FWS(Y; F_i, \mathcal{F}_{\setminus F_i}) + I(Y; F_i)$) and the $FWR(Y|F_i, \mathcal{F}_{\setminus F_i})$ is the unique information contributed by the FOI. More formally: $FWS(Y; F_i, \mathcal{F}_{\setminus F_i}) + I(Y; F_i) - FWR(Y|F_i, \mathcal{F}_{\setminus F_i}) = I(Y; \mathcal{F}_{\setminus F_i}, F_i) - I(Y; \mathcal{F}_{\setminus F_i})$.*

Proof. See Appendix B.1.

In Theorem 1, we have demonstrated that, the difference between the total information, and our definition of feature-wise redundancy $FWR(Y|F_i, \mathcal{F}_{\setminus F_i})$, is the non-redundant information gained by adding F_i to the set $\mathcal{F}_{\setminus F_i}$ (labelled as unique information in Figure 1). It follows that, we have

²Some prior knowledge of MI, synergy and redundancy are assumed throughout. If the reader is unfamiliar with these concepts, we refer them to Appendix A.

developed a consistent theory of feature-wise PID. Therefore, the presentation of the bars highlighted in Figure 1 is not only characterized by its interpretability but also its precise mathematical meaning.

5 Method

Throughout the remainder, the ability to calculate the MI (particularly $I(Y; F_i)$) is assumed. Consequently, the primary objective is to illustrate how we calculate both FWS and FWR. Specifically, we do this in two distinct steps. We introduce $\theta(Y; F_i, F_j, \mathcal{F}_{\setminus\{F_i, F_j\}})$, a measure that can provably detect both $FWR(Y|F_i, \mathcal{F}_{\setminus F_i})$ and $FWS(Y; F_i, \mathcal{F}_{\setminus F_i})$. With $\theta(Y; F_i, F_j, \mathcal{F}_{\setminus\{F_i, F_j\}})$ at its foundation, we then develop the PIDF algorithm.

5.1 Mutual Information Based Measure

The most desirable property of a measure to be used in PIDF would be if it could identify both $FWR(Y|F_i, \mathcal{F}_{\setminus F_i})$ and $FWS(Y; F_i, \mathcal{F}_{\setminus F_i})$ as defined earlier. Consequently, our measure takes the following form:

$$\theta(Y; F_i, F_j, \mathcal{F}_{\setminus\{F_i, F_j\}}) = (I(Y; F_i, \mathcal{F}_{\setminus F_i}) - I(Y; \mathcal{F}_{\setminus F_i})) - (I(Y; F_i, \mathcal{F}_{\setminus\{F_i, F_j\}}) - I(Y; \mathcal{F}_{\setminus\{F_i, F_j\}})).$$

$\theta(Y; F_i, F_j, \mathcal{F}_{\setminus\{F_i, F_j\}})$ quantifies how FNOI (F_j) affects the FOI's (F_i) ability to reduce the uncertainty of the target. This measure can quantify both synergy and redundancy according to the synergy redundancy index [Chechik et al., 2001], and our earlier definitions. To make this explicit, we present the following theorem:

Theorem 2: *If $\theta(Y; F_i, F_j, \mathcal{F}_{\setminus\{F_i, F_j\}}) > 0$, FNOI F_j is synergistic, more formally: $\theta(Y; F_i, F_j, \mathcal{F}_{\setminus\{F_i, F_j\}}) > 0 \Leftrightarrow Syn(Y; F_i, \mathcal{F}_{\setminus F_i}) > Syn(Y; F_i, \mathcal{F}_{\setminus\{F_i, F_j\}})$. Meanwhile, if $\theta(Y; F_i, F_j, \mathcal{F}_{\setminus\{F_i, F_j\}}) < 0$, FNOI F_j is redundant, more formally: $\theta(Y; F_i, F_j, \mathcal{F}_{\setminus\{F_i, F_j\}}) < 0 \Leftrightarrow CR(Y|F_i, \mathcal{F}_{\setminus F_i}) > CR(Y|F_i, \mathcal{F}_{\setminus\{F_i, F_j\}})$.*

Proof. See Appendix B.2.

5.2 Partial Information Decomposition of Features

In this section, we provide a description of PIDF. To do this, we first introduce a weak assumption under which we can prove that the MI between the FOI and an FNOI can be used as an indicator of redundancy. This theorem underpins the design of the PIDF paradigm. We conclude the section discussing the practical application of PIDF, also in terms of interpretability.

Preliminaries. In the previous section, we presented a measure that provably increases as synergy increases and, simultaneously, decreases as redundancy increases. Consequently, to find FWS and FWR we simply need to maximize $\theta(Y; F_i, F_j, \mathcal{F}_{\setminus\{F_i, F_j\}})$ across all possible subsets to find \mathcal{P}^{ms} . However, this is computationally inefficient. To overcome expensive subset searches dual methods have been proposed. Existing methods either, approximate the search [Covert et al., 2020, Chen et al., 2020, Yamada et al., 2020, Catav et al., 2021, Panda et al., 2021, Covert et al., 2023], or make an assumption about the data [Janssen et al., 2023, Westphal et al., 2024]. In this section, we take the latter approach. Our assumption involves limiting the complexity with which FNOIs can combine to provide redundant information regarding the FOI. In particular, we assume that a FNOI ($F_j \in \mathcal{F}_{\setminus F_i}$) may not combine with other FNOIs ($\mathcal{P} \in \mathcal{P}(\mathcal{F}_{\setminus F_i})$) synergistically to give redundant information regarding the FOI (F_i), more formally: $I(F_i; \mathcal{P}_{\setminus F_j}) + I(F_i; F_j) \geq I(F_i; \mathcal{P})$. This weak assumption was verified throughout our experimental evaluation, while also greatly simplifying the final implementation of PIDF. In this case, an FNOI can only be redundant due to a non-negative MI with the FOI. We now prove this result, showing that, given our assumption, $I(F_i; F_j)$ becomes a useful indicator as to whether F_j is redundant or synergistic.

Theorem 3: *The upper and lower bounds of $\theta(Y; F_i, F_j, \mathcal{F}_{\setminus\{F_i, F_j\}})$ are a function of the mutual information between the FOI and FNOI ($I(F_i; F_j)$). More formally: $2H(F_i) - I(F_i; F_j) \geq \theta(Y; F_i, F_j, \mathcal{F}_{\setminus\{F_i, F_j\}}) \geq -I(F_i; F_j)$.*

Proof. See Appendix B.3.

The above states that, the lower bound of our measure is $-I(F_i; F_j)$. Given we have shown that if $\theta(Y; F_i, F_j, \mathcal{F}_{\setminus\{F_i, F_j\}}) < 0$ the FNOI F_j is redundant, it is reasonable to use $I(F_i; F_j)$ as an

indicator of redundancy. Meanwhile, the upper bound is also a function of $-I(F_i; F_j)$. This indicates the inverse, that FNOI with low values of $I(F_i; F_j)$ are more likely to be synergistic. As first introduced in Section 4, to derive FWS and FWR we require the set of maximum synergy $\mathcal{P}^{m.s}$, which can concurrently be viewed as a set devoid of redundancy. Consequently, we aim to design PIDF so that it detects and removes redundant features. Meanwhile, in this paragraph we have proven that our assumption restricts cases of redundancy to those caused by non-negative MI between features. Consequently, under our assumption we derive the set of maximum synergy using the PIDF algorithm as defined in the following paragraph.

Description of PIDF. To begin, we calculate $I(Y; F_i)$. Following this, we rank the FNOI in descending order of $I(F_i, F_j)$ as, according to our assumption, this indicates redundancy. We then iterate through the FNOI checking if they are truly redundant according to $\theta(Y; F_i, F_j, \mathcal{F}_{\setminus\{F_i, F_j\}})$ (the box titled ‘PIDF Algorithm’ in Figure 1 illustrates this process). If so, they can be removed from the set $\mathcal{F}_{\setminus F_i}$. We continue to remove FNOIs until the remainder are no longer redundant; indicating the discovery of the set of maximum synergy. By repeating these steps for all $F_i \in \mathcal{F}$ we derive the FWS, FWR, and MI for each feature as desired. For an algorithmic definition of this process, please refer to Algorithm C.1 in Appendix C, and, for an example calculation, Appendix D.

Adapting PIDF for varying estimates. Unless restricting oneself to discreet data, exact calculations of MI are not possible. Consequently, we estimate it using methods outlined by Belghazi et al. [2018]. These estimates can randomly fluctuate, which can lead to the erroneous identification of redundant FNOIs during the evaluation of line 7 in Algorithm C.1. To overcome this, when estimating any MI (or MI based measure), the process is repeated multiple times. For a FNOI to then be considered redundant there has to be a 95% certainty that $\theta(Y; F_i, F_j, \mathcal{F}_{\setminus\{F_i, F_j\}}) < 0$. Otherwise, the feature is classed as non-redundant.

Interpretability of PIDF FWR. We assume that FNOIs can provide redundant information regarding the FOI, provided that it is not synergistic. This implies that the total redundant information in the FNOIs must be a linear combination of individual contributions. Consequently, we need not present redundancy as just one bar, but rather as a stack of all the individual contributions from all the redundant FNOIs. As a concrete example, consider the diagram labelled as MSQ in Figure 2. For feature F_0 , the FWR on the right-hand side of the total information is not represented by a single bar, but rather as one composed by multiple stacked redundant contributions from individual FNOIs. The possibility of discriminating between the different redundant contributions through PIDF allows for better overall interpretability, by highlighting which FNOIs are the most redundant.

5.3 Partial Information Decomposition for Feature Selection

We now provide a procedure for feature selection based on the output of PIDF. First of all, we select all features with a non-redundant contribution, i.e., any features whose total information exceeds their FWR. We then rank the remaining features by their total information and check in descending order if any of their redundant FNOIs, which according to our assumption are those with a non-negligible MI with the FOI, have already been selected. If so, we do not add this FOI; otherwise, we proceed to add it. As was the case for PIDF, exceeding thresholds must be done with a minimum of 95% certainty, where the MIs at the basis of these calculations have been estimated using multiple random seeds. The steps of the procedure are detailed in Algorithm 2 (Appendix C). For a fully worked example of these steps, please refer to Appendix D.

6 Experimental Evaluation

6.1 PIDF for Data Intepretability

We begin by evaluating our method’s ability to explain data, comparing it to three pre-existing baselines: UEFI Janssen et al. [2023], MCI Catav et al. [2021] and PI Breiman [2001]. For a full discussion of the hyperparameters used for all methods please refer to Appendix E. Furthermore, for a detailed example of how to interpret the results of PIDF please refer to Appendix F.

6.1.1 Synthetic Datasets

We now discuss the results obtained when applying PIDF to synthetic datasets. The first three of these datasets were designed to highlight how current methods fail to properly address the questions introduced in Section 2. The following five are taken from pre-existing works. A description of these datasets can be found in Appendix G.

Redundant variables question (RVQ) dataset. We now design an extremely simple dataset to demonstrate our method’s ability to answer the RVQ, as introduced in Section 2. The dataset is designed such that $F_1 \equiv F_2$, meaning these two features are fully redundant with respect to one another, as revealed by PIDF in Figure 2. Meanwhile, using MCI one would assume that we have three features of equal importance, without knowledge of the redundancy.

Synergistic variables question (SVQ) dataset.

We now present the evaluation conducted to answer the SVQ introduced in Section 2. In this dataset, the target is formed by the synergistic combination of the two features. This is indicated by the FNOI subscripts in the synergy bar for features F_0 and F_1 , as shown in Figure 2³. We observe that only PIDF reveals that F_0 combines with F_1 synergistically.

Multiple subsets question (MSQ) dataset.

This dataset is characterized by redundancy between the subset $\{F_1, F_2\}$ and the variable F_0 . In Figure 2, we observe that our method again resolves the complex relationships correctly.

Wollstadt toy dataset (WT). The Wollstadt toy example is characterized by three variables. Two of which are informative, while one is fully redundant. Of these informative variables, one provides ‘conventional’ information while the other provides synergistic information. The method developed in Wollstadt et al. [2023] was able to identify both the informative variables, while simultaneously highlighting that one of these variables was only informative in combination. In Figure 3, we observe that not only does PIDF reveal the interactions as they were in Wollstadt et al. [2023], but it also illustrates that F_1 provides more information than F_2 , although it is fully redundant.

TERC-1 & TERC-2. These datasets, introduced by Westphal et al. [2024], are characterized by features that are simultaneously both redundant and synergistic, as illustrated in Figure 3. Moreover, through the labels of the green and purple bars, one can understand with which FNOIs these interactions occur.

UMFI blood relation dataset (UBR). Janssen et al. [2023] used the UBR dataset to demonstrate that their method only assigns non-negligible importances to features that are related to the target via a directed path or causal ancestor [Pearl, 1986]. Despite neither F_1 nor F_2 satisfying these conditions, methods from a previous work [Catav et al., 2021] still assigned them as important. However, PIDF avoids these issues. Additionally, unlike UMFI, PIDF reveals that the information provided in F_2 is redundant with respect to F_3 .

Synthetic genes dataset (SG). Our final synthetic dataset was developed in Anastassiou [2007] to demonstrate that two genes could interact synergistically, while others are redundant. We observe that our method, similarly to the PID analysis in Anastassiou [2007], has the capability to reveal such

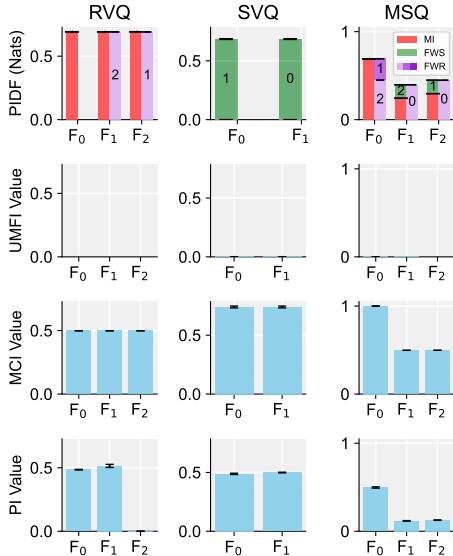


Figure 2: Comparison of feature importance indicators using synthetic datasets for the analysis of RVQ, SVQ and MSQ.

³We indicate the FNOI subscripts in black if inside the bars. If there is not sufficient space, the numbers are located above or to the right, and their color matches their corresponding bar.

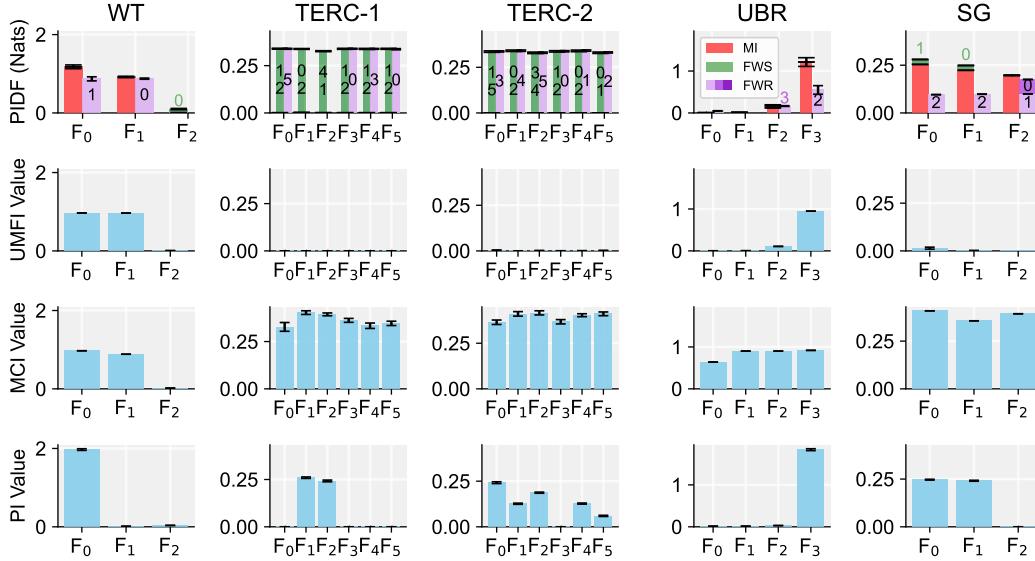


Figure 3: Comparison of feature importance indicators using synthetic datasets from the literature.

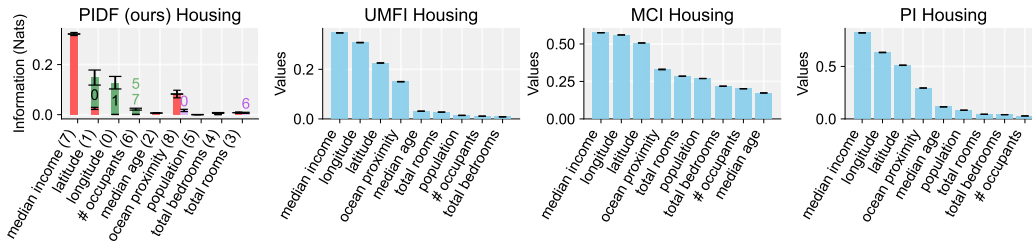


Figure 4: Comparison of feature importance indicators applied to the California housing dataset.

relationships. However, in the preceding section, we will show our methods scalability, by applying it to real genetics datasets.

6.1.2 Real-World Datasets

California housing dataset. In this section, we use our method to explain the well adopted California housing dataset. In Figure 4, we observe that the longitude and latitude combine synergistically. Alone, neither the longitude nor the latitude have great predictive power of housing prices. On the contrary, when considered together, these variables reveal an exact location, and become a very useful indicator. Another interesting feature of these results is that the ocean proximity is only redundant with respect to the longitude, as the coast is to the east. Other methods are unable to reveal such relationships. For extra experiments on classic ML datasets, please refer to Appendix I.

BRCA dataset. We now demonstrate the efficacy of our method in describing the relationships between genes in the BRCA dataset (available here: <https://portal.gdc.cancer.gov/projects/TCGA-BRCA>) [Tomczak et al., 2015, Ashton et al., 2018]. This dataset details the RNA expression levels of many genes in patients with and without breast cancer. Of these genes, 10 are known chemically to cause cancer. Previously, those using this dataset to study feature importance [Catav et al., 2021, Janssen et al., 2023] have aimed to develop methods which identify these as the 10 most important genes. In this study, we instead focus on how these 10 genes interact to cause breast cancer. In Figure 5, we observe that CDK6 interacts synergistically with multiple genes. This is because CDK6 is known to regulate gene expression levels in the cell, which in turn promotes or inhibits division [Nebenfuhr et al., 2020, Goel et al., 2022]. Consequently, in a healthy cell CDK6 expression levels are closely correlated with those of the genes it regulates. On the contrary, this is not the case in cancerous cells [Malumbres and Barbacid, 2009], where the CDK6 present becomes overactive, leading to expression levels that greatly exceed what is typically expected. PIDF, unlike

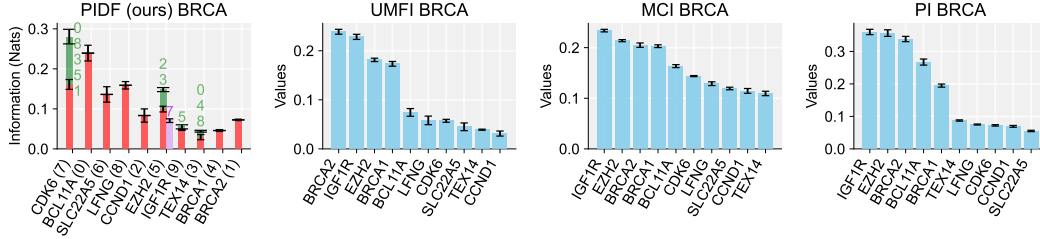


Figure 5: Comparison of feature importance methods ability to explain how genes interact to cause cancer in the BRCA dataset.

the baselines, indicates that we require the expression levels of both CDK6 and the genes it regulates to predict cancer, which is consistent with the overactive CDK6 hypothesis.

Neuron growth experiment. In this experiment, we study the information-theoretic quantities that characterize the spiking interactions that form within a dissociated neural culture over 33 days. Full details of the dataset are available in Appendix H. We now discuss the results presented in Figure 6, where we observe the average FWR, FWS and MI for each neuron at each day over different neuron subsets. A pronounced initial increase in redundancy is followed by a decrease.

This phenomenon aligns with the principles of Hebbian theory [Hebb, 2005]: the initial surge in redundancy can be attributed to the exploratory phase of neural connections, during which abundant synaptic connections are established randomly. Subsequently, synaptic links between neurons that do not exhibit synchronized firing patterns are pruned. This adaptive reconfiguration of the network results in not only a reduction in the observed redundancy, but also a gradual increase in synergy and mutual information.

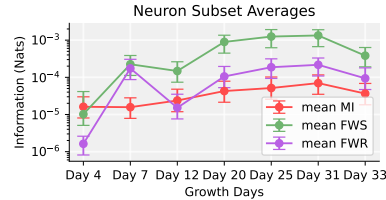


Figure 6: Average FWR, FWS, and MI per neuron as synaptic connections are re-established in dissociated culture over 33 days.

6.2 PIDF for Feature Selection

Performance Evaluation. In Section 5.3, we developed a simple algorithm based on PIDF for feature selection. We now evaluate this technique. Each synthetic dataset in Section 6.1.1, characterized by certain relationships, has an associated set of optimal features. In this section, we verify our method selects this optimal subset. We adopt the methods described in Wollstadt et al. [2023], [Westphal et al., 2024] (TERC), and Breiman [2001] (PI) as baselines. In Table 1 we observe that PIDF selects the optimal number of features for all the datasets investigated; however, this is not the case for the baselines. The method developed in Wollstadt et al. [2023] fails to recognize fully synergistic variables as important (hence, the poor results achieved on the SVQ, TERC-1, and TERC-2 datasets). Meanwhile, TERC is not able to address the MSQ due to its inability to rank features based on their total information.

Table 1: Number of true positive (TP), false positive (FP), true negative (TN), and false negative (FN) features selected using each method. Red values represent optimal performance, and confidence intervals were omitted since negligible variations were observed.

Dataset	PIDF				Wollstadt				TERC				PI			
	TP	FP	TN	FN	TP	FP	TN	FN	TP	FP	TN	FN	TP	FP	TN	FN
RVQ	2	0	1	0	2	0	1	0	2	0	1	0	2	0	1	0
SVQ	2	0	0	0	0	0	0	2	2	0	0	0	2	0	0	0
MSQ	1	0	2	0	1	0	2	0	0	2	0	1	1	2	0	0
WT	2	0	1	0	2	0	1	0	2	0	1	0	2	0	1	0
TERC-1	3	0	3	0	0	0	3	3	3	0	3	0	2	0	3	1
TERC-2	3	0	3	0	0	0	3	3	3	0	3	0	3	3	0	0
UMFIBR	1	0	3	0	1	0	3	0	1	0	3	0	1	3	0	0
SG	3	0	0	0	3	0	0	0	3	0	0	0	2	0	0	1

7 Concluding Remarks

Summary of the Contributions. In this paper, we have presented PIDF, a novel paradigm for simultaneous data interpretability and feature selection based on per-feature synergy, redundancy and

mutual information. Through an extensive evaluation using both synthetic and real-world data, we have demonstrated its effectiveness in analyzing and interpreting systems characterized by complex interactions. As part of our research agenda, we plan to explore the potential of applying PIDF to open problems in a variety of scientific fields.

Limitations. The main limitation of PIDF is its temporal complexity, which scales as a function $\mathcal{O}(k^2)$, where k is the number of features. It is worth noting that it is not directly comparable with the other methods since it captures feature-wise synergistic interactions, an intrinsically computationally expensive task. Consequently, in order to scale-up to very-large feature spaces, it is necessary to adopt hierarchical solutions for the comparison of sets of variables in PIDF.

References

- Kjersti Aas, Martin Jullum, and Anders Løland. Explaining individual predictions when features are dependent: More accurate approximations to Shapley values. *Artificial Intelligence*, 298(4):103502, 2021.
- Dimitris Anastassiou. Computational analysis of the synergy among multiple interacting genes. *Molecular Systems Biology*, 3(1):83, 2007.
- Daniel W. Apley and Jingyu Zhu. Visualizing the effects of predictor variables in black box supervised learning models. *Journal of the Royal Statistical Society Series B*, 82(4):1059–1086, 2020.
- Berger Ashton et al. A comprehensive pan-cancer molecular study of gynecologic and breast cancers. *Cancer Cell*, 33(4):690–705.e9, 2018. ISSN 1535-6108.
- R. Battiti. Using mutual information for selecting features in supervised neural net learning. *IEEE Transactions on Neural Networks*, 5(4):537–550, 1994.
- Ishmael Belghazi, Sai Rajeswar, Aristide Baratin, R Devon Hjelm, and Aaron Courville. Mine: Mutual information neural estimation. In *ICML’18*, 2018.
- Nils Bertschinger, Johannes Rauh, Eckehard Olbrich, and Jürgen Jost. Shared information—new insights and problems in decomposing information in complex systems. In Thomas Gilbert, Markus Kirkilionis, and Gregoire Nicolis, editors, *ECS’12*, pages 251–269. Springer International Publishing, 2013.
- Leo Breiman. Random forests. *Machine Learning*, 45(1):5–32, 2001.
- Gavin Brown, Adam Pocock, Ming-Jie Zhao, and Mikel Luján. Conditional likelihood maximisation: A unifying framework for information theoretic feature selection. *Journal of Machine Learning Research*, 13(2):27–66, 2012.
- Amnon Catav, Boyang Fu, Yazeed Zoabi, Ahuva Libi Weiss Meilik, Noam Shomron, Jason Ernst, Sriram Sankararaman, and Ran Gilad-Bachrach. Marginal contribution feature importance - an axiomatic approach for explaining data. In *ICML’21*, 2021.
- Gal Chechik, Amir Globerson, M Anderson, E Young, Israel Nelken, and Naftali Tishby. Group redundancy measures reveal redundancy reduction in the auditory pathway. In *NeurIPS’01*, 2001.
- Hugh Chen, Joseph D. Janizek, Scott Lundberg, and Su-In Lee. True to the model or true to the data? *arXiv preprint arXiv:2006.16234*, 2020.
- Jianbo Chen, Le Song, Martin Wainwright, and Michael Jordan. Learning to explain: An information-theoretic perspective on model interpretation. In *ICML’18*, 2018.
- Shay Cohen, Gideon Dror, and Eytan Ruppin. Feature selection via coalitional game theory. *Neural Computation*, 19(8):1939–61, 2007.
- Ian C. Covert, Scott Lundberg, and Su-In Lee. Understanding global feature contributions with additive importance measures. In *NeurIPS’20*, 2020.
- Ian Connick Covert, Wei Qiu, Mingyu Lu, Na Yoon Kim, Nathan J White, and Su-In Lee. Learning to maximize mutual information for dynamic feature selection. In *ICML’23*, 2023.

- Dries Debeer and Carolin Strobl. Conditional permutation importance revisited. *BMC Bioinformatics*, 21(1):1–30, 07 2020.
- Aaron Fisher, Cynthia Rudin, and Francesca Dominici. All models are wrong, but many are useful: Learning a variable’s importance by studying an entire class of prediction models simultaneously. *Journal of Machine Learning Research*, 20(177):1–81, 2019.
- Christopher Frye, Colin Rowat, and Ilya Feige. Asymmetric Shapley Values: Incorporating Causal Knowledge into Model-Agnostic Explainability. In *NeurIPS’20*, 2020.
- Shuyang Gao, Greg Ver Steeg, and Aram Galstyan. Variational information maximization for feature selection. In *NeurIPS’16*, 2016.
- Shom Goel, Johann S Bergholz, and Jean J Zhao. Targeting CDK4 and CDK6 in cancer. *Nature Reviews Cancer*, 22(6):356–372, 2022.
- Virgil Griffith and Tracey Ho. Quantifying redundant information in predicting a target random variable. *Entropy*, 17(7):4644–4653, 2015.
- Virgil Griffith and Christof Koch. Quantifying synergistic mutual information. In *Guided Self-Organization: Inception*, pages 159–190. Springer, 2014.
- Donald Olding Hebb. *The organization of behavior: A neuropsychological theory*. Psychology Press, 2005.
- Joseph Janssen, Vincent Guan, and Elina Robeva. Ultra-marginal feature importance: Learning from data with causal guarantees. In *ICAIS’23*, 2023.
- Alon Keinan, Claus C. Hilgetag, Isaac Meilijson, and Eytan Ruppin. Causal localization of neural function: the Shapley value method. *Neurocomputing*, 58-60(3):215–222, 2004.
- Elizabeth Kumar, Suresh Venkatasubramanian, Carlos Scheidegger, and Sorelle A. Friedler. Problems with Shapley-Value-Based Explanations as Feature Importance Measures. In *ICML’20*, 2020.
- Yongchan Kwon and James Y Zou. WeightedSHAP: analyzing and improving Shapley based feature attributions. In *NeurIPS’22*, 2022.
- Chin Wa Lau, Chandra Nair, and David Ng. A mutual information inequality and some applications. *IEEE Transactions on Information Theory*, 69(10), 2023.
- Marcos Malumbres and Mariano Barbacid. Cell cycle, cdks and cancer: a changing paradigm. *Nature Reviews Cancer*, 9(3):153–166, 2009.
- Young-Il Moon, Balaji Rajagopalan, and Upmanu Lall. Estimation of mutual information using kernel density estimators. *Physical Review E*, 52(3):2318–2321, 1995.
- Sofie Nebenfuehr, Karoline Kollmann, and Veronika Sexl. The role of CDK6 in cancer. *International Journal of Cancer*, 147(11):2988–2995, 2020.
- Milan Paluš. Detecting nonlinearity in multivariate time series. *Physics Letters A*, 213(3):138–147, 1996.
- Pranoy Panda, Sai Srinivas Kancheti, and Vineeth N Balasubramanian. Instance-wise causal feature selection for model interpretation. In *CVPR’21*, 2021.
- Liam Paninski. Estimation of entropy and mutual information. *Neural Computation*, 15(6):1191–1253, 2003.
- Judea Pearl. Fusion, propagation, and structuring in belief networks. *Artificial Intelligence*, 29(3): 241–288, 1986.
- Hanchuan Peng, Fuhui Long, and Chris Ding. Feature selection based on mutual information criteria of max-dependency, max-relevance, and min-redundancy. *IEEE Transactions on Pattern Analysis and Machine Intelligence*, 27(8):1226–1238, 2005.

- Ben Poole, Sherjil Ozair, Aaron Oord, Alexander Alemi, and George Tucker. On variational bounds of mutual information. In *ICML'19*, 2019.
- Shachar Schnapp and Sivan Sabato. Active feature selection for the mutual information criterion. In *AAAI'21*, 2021.
- Elad Schneidman, Susanne Still, Michael J Berry, William Bialek, et al. Network information and connected correlations. *Physical review letters*, 91(23):238701, 2003.
- Claude E Shannon. A mathematical theory of communication. *The Bell System Technical Journal*, 27(3):379–423, 1948.
- Bastian Steudel and Nihat Ay. Information-theoretic inference of common ancestors. *Entropy*, 17(4):2304–2327, 2015.
- Nicholas M Timme and Christopher Lapish. A tutorial for information theory in neuroscience. *eNeuro*, 5(3), 2018.
- Katarzyna Tomczak, Patrycja Czerwińska, and Maciej Wiznerowicz. Review The Cancer Genome Atlas (TCGA): an immeasurable source of knowledge. *Contemporary Oncology/Współczesna Onkologia*, 2015(1):68–77, 2015.
- Aaron van den Oord, Yazhe Li, and Oriol Vinyals. Representation learning with contrastive predictive coding. *arXiv preprint arXiv:1807.03748*, 2019.
- Daniel A Wagenaar, Jerome Pine, and Steve M Potter. An extremely rich repertoire of bursting patterns during the development of cortical cultures. *BMC Neuroscience*, 7(1):1–18, 2006.
- Ethan Weinberger, Ian Covert, and Su-In Lee. Feature selection in the contrastive analysis setting. In *NeurIPS'23*, 2023.
- Charles Westphal, Stephen Hailes, and Mirco Musolesi. Information-theoretic state variable selection for reinforcement learning. *arXiv preprint arXiv:2401.11512*, 2024.
- Paul L. Williams and Randall D. Beer. Nonnegative decomposition of multivariate information. *arXiv preprint arXiv:1004.2515*, 2010.
- Patricia Wollstadt, Sebastian Schmitt, and Michael Wibral. A rigorous information-theoretic definition of redundancy and relevancy in feature selection based on (partial) information decomposition. *Journal of Machine Learning Research*, 24(131):1–44, 2023.
- Yutaro Yamada, Ofir Lindenbaum, Sahand Negahban, and Yuval Kluger. Feature selection using stochastic gates. In *ICML'20*, 2020.
- Sepehr Zadeh, Mehrdad Ghadiri, Vahab Mirrokni, and Morteza Zadimoghaddam. Scalable feature selection via distributed diversity maximization. In *AAAI'17*, 2017.

A Key Information-Theoretic Concepts

We now review key information-theoretic concepts used in the main article.

A.1 Mutual Information

MI aims to describe how much information two variables share. Formally it is written as follows: $I(X; Z) = H(X) - H(X|Z)$. This quantifies the number of bits of information you learn about X by observing Z . MI is the predominant metric used when ranking features [Battiti, 1994, Peng et al., 2005, Brown et al., 2012, Schnapp and Sabato, 2021], based on its ability to capture non-linear relationships. Unless restricting oneself to unrealistic scenarios, calculating MI is often intractable. Consequently, a variety of methods have been derived to estimate it [Moon et al., 1995, Paninski, 2003, Belghazi et al., 2018, van den Oord et al., 2019, Poole et al., 2019]. Throughout this paper, we deploy the method described in Belghazi et al. [2018] due to its applicability to discrete and continuous data.

A.2 Synergy of Sets

Synergy, characterizes the additional information obtained by evaluating variables collectively rather than individually. We present the following formal definition, as developed by Anastassiou [2007]:

$$Syn(Z; X_1, X_2 \dots X_N) = I(Z; X_1, X_2 \dots X_N) - \sum_{i=1}^N I(Z; X_i). \quad (1)$$

Synergistic interactions have been shown to invalidate the feature importance scores assigned by correlation based methods. For illustration, let us consider two features (F_1 and F_2). Alone, they provide no information about the target $I(Y; F_1) = I(Y; F_2) = 0$. However, when combined, they are completely informative $I(Y; F_1, F_2) = H(Y)$. This can be achieved by forming Y by combining F_1 and F_2 via an XOR function. Now, let us suppose we use an MI-based approach to rank the features, such as that used by Wollstadt et al. [2023]. We would identify both features F_1 and F_2 as completely uninformative, a result that is not representative of the underlying data [Brown et al., 2012, Zadeh et al., 2017]. Shapley-value based approaches solve such issues; however, these methods are characterized by the searching of subset permutations, which is a computationally complex task. Of these methods, many restrict the levels of computation required by using gradient descent guided subset search [Covert et al., 2020, Chen et al., 2020, Yamada et al., 2020, Catav et al., 2021, Panda et al., 2021, Covert et al., 2023]. Nonetheless, what these methods gain in efficiency, is lost in provable optimality.

A.3 Redundancy of Sets

Redundancy [Frye et al., 2020, Kumar et al., 2020, Debeer and Strobl, 2020] aims to quantify the disparity between the theoretically maximal uncertainty of a variable ensemble and its actual uncertainty. High levels of redundancy suggest a significant difference, while low levels indicate the contrary. Throughout this paper, our interest lies in the redundancy of our feature set with respect to our target variable. Consequently, we only refer to conditional redundancy, which is defined as:

$$CR(Z|X_1; X_2; \dots X_N) = H(Z|X_1, X_2, \dots X_N) - \sum_{i=1}^N H(Z|X_i). \quad (2)$$

Equation 2 is a variation of the conditional redundancy originally introduced by Schneidman et al., and implies a similar notion to the non-conditional redundancy [Schneidman et al., 2003]. Except here, we quantify the difference between the maximum and the true reduction in uncertainty of the target variable caused by an ensemble. It has been shown, both theoretically and empirically, that Shapley value based feature importances behave non-optimally in the presence of perfect redundancies [Frye et al., 2020, Kumar et al., 2020, Debeer and Strobl, 2020].

B Proofs

B.1 Proof of Theorem 1

Proof. We now prove Theorem 1.

$$\begin{aligned}
& FWS(Y; F_i, \mathcal{F}_{\setminus F_i}) + I(Y; F_i) - FWR(Y|F_i, \mathcal{F}_{\setminus F_i}) \\
&= \max_{\mathcal{P}^{ms} \in \mathcal{P}(\mathcal{F}_{\setminus F_i})} (I(Y; F_i, \mathcal{P}_{\setminus F_i}^{ms}) - I(Y; \mathcal{P}_{\setminus F_i}^{ms})) - FWR(Y|F_i, \mathcal{F}_{\setminus F_i}) \\
&\text{(Via our definition of FWS and cancelling } I(Y; F_i)\text{'s)} \\
&= - \min_{\mathcal{P}^{ms} \in \mathcal{P}(\mathcal{F}_{\setminus F_i})} (H(Y|F_i, \mathcal{P}_{\setminus F_i}^{ms}) - H(Y|\mathcal{P}_{\setminus F_i}^{ms})) - FWR(Y|F_i, \mathcal{F}_{\setminus F_i}) \\
&\text{(By } \max(f(x)) = -\min(-f(x))\text{, and cancelling } H(Y)\text{'s)} \\
&= - \min_{\mathcal{P}^{ms} \in \mathcal{P}(\mathcal{F}_{\setminus F_i})} (H(Y|F_i, \mathcal{P}_{\setminus F_i}^{ms}) - H(Y|\mathcal{P}_{\setminus F_i}^{ms})) - (H(Y|F_i, \mathcal{F}_{\setminus F_i}) - H(Y|\mathcal{F}_{\setminus F_i})) \quad (3) \\
&+ \min_{\mathcal{P}^{ms} \in \mathcal{P}(\mathcal{F}_{\setminus F_i})} ((H(Y|F_i, \mathcal{P}^{ms}) - H(Y|\mathcal{P}^{ms}))) \\
&\text{(By our definition of FWR, and cancelling } H(Y|F_i)\text{)} \\
&= H(Y|\mathcal{F}_{\setminus F_i}) - H(Y|F_i, \mathcal{F}_{\setminus F_i}) \quad \text{(1st and 3rd terms cancel)} \\
&= I(Y; F_i, \mathcal{F}_{\setminus F_i}) - I(Y; \mathcal{F}_{\setminus F_i}) \quad \text{(By addition of } H(Y) - H(Y) = 0\text{)}
\end{aligned}$$

B.2 Proof of Theorem 2

Proof. To prove Theorem 2 we begin by showing $\theta(Y; F_i, F_j, \mathcal{F}_{\setminus \{F_i, F_j\}}) > 0 \Leftrightarrow \text{Syn}(Y; F_i, \mathcal{F}) > \text{Syn}(Y; F_i, \mathcal{F}_{\setminus \{F_i, F_j\}})$.

$$\begin{aligned}
& \theta(Y; F_i, F_j, \mathcal{F}_{\setminus \{F_i, F_j\}}) > 0 \\
& I(Y; F_i, \mathcal{F}_{\setminus F_i}) - I(Y; \mathcal{F}_{\setminus F_i}) > I(Y; F_i, \mathcal{F}_{\setminus \{F_i, F_j\}}) - I(Y; \mathcal{F}_{\setminus \{F_i, F_j\}}) \\
& I(Y; F_i, \mathcal{F}_{\setminus F_i}) - I(Y; \mathcal{F}_{\setminus F_i}) - I(Y; F_i) > I(Y; F_i, \mathcal{F}_{\setminus \{F_i, F_j\}}) - I(Y; \mathcal{F}_{\setminus \{F_i, F_j\}}) - I(Y; F_i) \\
& \quad \text{(subtracting } I(Y; F_i)\text{ from both sides)} \\
& \text{Syn}(Y; F_i, \mathcal{F}_{\setminus F_i}) > \text{Syn}(Y; F_i, \mathcal{F}_{\setminus \{F_i, F_j\}}) \quad \text{(by synergy definition).} \quad (4)
\end{aligned}$$

To complete the proof we show $\theta(Y; F_i, F_j, \mathcal{F}_{\setminus \{F_i, F_j\}}) < 0 \Leftrightarrow FWR(Y|F_i, \mathcal{F}_{\setminus F_i}) > FWR(Y|F_i, \mathcal{F}_{\setminus \{F_i, F_j\}})$.

$$\begin{aligned}
& \theta(Y; F_i, F_j, \mathcal{F}_{\setminus \{F_i, F_j\}}) < 0 \\
& I(Y; F_i, \mathcal{F}_{\setminus F_i}) - I(Y; \mathcal{F}_{\setminus F_i}) < I(Y; F_i, \mathcal{F}_{\setminus \{F_i, F_j\}}) - I(Y; \mathcal{F}_{\setminus \{F_i, F_j\}}) \\
& H(Y) - H(Y|F_i, \mathcal{F}_{\setminus F_i}) - H(Y) + H(Y|\mathcal{F}_{\setminus F_i}) < H(Y) - H(Y|F_i, \mathcal{F}_{\setminus \{F_i, F_j\}}) - H(Y) \\
& \quad + H(Y|\mathcal{F}_{\setminus \{F_i, F_j\}}) \\
& -H(Y|F_i, \mathcal{F}_{\setminus F_i}) + H(Y|\mathcal{F}_{\setminus F_i}) < -H(Y|F_i, \mathcal{F}_{\setminus \{F_i, F_j\}}) \\
& \quad + H(Y|\mathcal{F}_{\setminus \{F_i, F_j\}}) \\
& H(Y|F_i) - H(Y|F_i, \mathcal{F}_{\setminus F_i}) + H(Y|\mathcal{F}_{\setminus F_i}) < H(Y|F_i) - H(Y|F_i, \mathcal{F}_{\setminus \{F_i, F_j\}}) + H(Y|\mathcal{F}_{\setminus \{F_i, F_j\}}) \\
& \quad \text{(adding } H(Y|F_i)\text{ to each side)} \\
& -H(Y|F_i) + H(Y|F_i, \mathcal{F}_{\setminus F_i}) - H(Y|\mathcal{F}_{\setminus F_i}) > -H(Y|F_i) + H(Y|F_i, \mathcal{F}_{\setminus \{F_i, F_j\}}) - \\
& \quad H(Y|\mathcal{F}_{\setminus \{F_i, F_j\}}) \quad \text{(multiply by -1),} \\
& CR(Y|F_i, \mathcal{F}_{\setminus F_i}) > CR(Y|F_i, \mathcal{F}_{\setminus \{F_i, F_j\}}) \\
& \quad \text{(by definition of redundancy).} \quad (5)
\end{aligned}$$

B.3 Proof of Theorem 3

Proof. We begin by proving the lower bound. This proof shares the first few steps with those described in Steudel and Ay [2015], Lau et al. [2023], Janssen et al. [2023], before we then use our assumption

to complete the proof.

$$\begin{aligned}
& I(Y; F_i, \mathcal{F}_{\setminus\{F_i, F_j\}}, F_j) - I(Y; \mathcal{F}_{\setminus\{F_i, F_j\}}, F_j) \\
&= I(Y; F_i | \mathcal{F}_{\setminus\{F_i, F_j\}}, F_j) + I(Y; \mathcal{F}_{\setminus\{F_i, F_j\}}, F_j) - I(Y; \mathcal{F}_{\setminus\{F_i, F_j\}}, F_j) \\
&\quad \text{(via the chain rule)} \\
&= I(F_i; Y | \mathcal{F}_{\setminus\{F_i, F_j\}}, F_j) \\
&\quad \text{(via symmetry)} \\
&= I(F_i; Y, \mathcal{F}_{\setminus\{F_i, F_j\}}, F_j) - I(F_i; \mathcal{F}_{\setminus\{F_i, F_j\}}, F_j) \\
&\quad \text{(via the chain rule)} \\
&\geq I(F_i; Y, \mathcal{F}_{\setminus\{F_i, F_j\}}) - I(F_i, \mathcal{F}_{\setminus\{F_i, F_j\}}) - I(F_i, F_j) \\
&\quad \text{(via the monotonicity of MI and our assumption)} \\
&\geq I(F_i; Y | \mathcal{F}_{\setminus\{F_i, F_j\}}) + I(F_i; \mathcal{F}_{\setminus\{F_i, F_j\}}) - I(F_i, \mathcal{F}_{\setminus\{F_i, F_j\}}) - I(F_i, F_j) \\
&\quad \text{(via the chain rule)} \\
&\geq I(Y; F_i | \mathcal{F}_{\setminus\{F_i, F_j\}}) - I(F_i, F_j) \\
&\quad \text{(via symmetry)} \\
&\geq I(Y; F_i, \mathcal{F}_{\setminus\{F_i, F_j\}}) - I(Y; \mathcal{F}_{\setminus\{F_i, F_j\}}) - I(F_i, F_j) \\
&\quad \text{(via chain rule)} \\
\theta(Y; F_i, F_j, \mathcal{F}_{\setminus\{F_i, F_j\}}) &\geq -I(F_i, F_j)
\end{aligned} \tag{6}$$

We now provide the upper bound to complete the proof.

$$\begin{aligned}
& I(Y; F_i, \mathcal{F}_{\setminus\{F_i, F_j\}}, F_j) - I(Y; \mathcal{F}_{\setminus\{F_i, F_j\}}, F_j) \\
&= I(Y; F_i | \mathcal{F}_{\setminus\{F_i, F_j\}}, F_j) + I(Y; \mathcal{F}_{\setminus\{F_i, F_j\}}, F_j) - I(Y; \mathcal{F}_{\setminus\{F_i, F_j\}}, F_j) \\
&\quad \text{(via the chain rule)} \\
&= I(F_i; Y | \mathcal{F}_{\setminus\{F_i, F_j\}}, F_j) \quad \text{(via symmetry)} \\
&= I(F_i; Y, \mathcal{F}_{\setminus\{F_i, F_j\}}, F_j) - I(F_i; \mathcal{F}_{\setminus\{F_i, F_j\}}, F_j) \quad \text{(via the chain rule)} \\
&\leq I(F_i; Y, \mathcal{F}_{\setminus\{F_i, F_j\}}, F_j) - I(F_i; F_j) \quad \text{(via the monotonicity of MI)} \\
&\leq I(F_i; Y, F_j | \mathcal{F}_{\setminus\{F_i, F_j\}}) + I(F_i; Y, \mathcal{F}_{\setminus\{F_i, F_j\}}) - I(F_i; F_j) \\
&\quad \text{(via the chain rule)} \\
&\leq I(F_i; Y, F_j | \mathcal{F}_{\setminus\{F_i, F_j\}}) + I(F_i; Y | \mathcal{F}_{\setminus\{F_i, F_j\}}) + I(F_i; \mathcal{F}_{\setminus\{F_i, F_j\}}) - I(F_i; F_j) \\
&\quad \text{(via the chain rule)} \\
&\leq I(F_i; Y, F_j | \mathcal{F}_{\setminus\{F_i, F_j\}}) + I(Y; F_i | \mathcal{F}_{\setminus\{F_i, F_j\}}) + I(F_i; \mathcal{F}_{\setminus\{F_i, F_j\}}) - I(F_i; F_j) \\
&\quad \text{(via symmetry)} \\
&\leq I(F_i; Y, F_j | \mathcal{F}_{\setminus\{F_i, F_j\}}) + I(Y; F_i, \mathcal{F}_{\setminus\{F_i, F_j\}}) \\
&\quad - I(Y; \mathcal{F}_{\setminus\{F_i, F_j\}}) + I(F_i; \mathcal{F}_{\setminus\{F_i, F_j\}}) - I(F_i; F_j) \\
&\quad \text{(via the chain rule)} \\
&\leq I(F_i; Y, F_j | \mathcal{F}_{\setminus\{F_i, F_j\}}) + \theta(Y; F_i, \mathcal{F}_{\setminus\{F_i, F_j\}}) + I(F_i; \mathcal{F}_{\setminus\{F_i, F_j\}}) - I(F_i; F_j) \\
&\quad \text{(via the chain rule)} \\
\theta(Y; F_i, F_j, \mathcal{F}_{\setminus\{F_i, F_j\}}) &\leq I(F_i; Y, F_j | \mathcal{F}_{\setminus\{F_i, F_j\}}) + I(F_i; \mathcal{F}_{\setminus\{F_i, F_j\}}) - I(F_i; F_j) \\
&\leq 2H(F_i) - I(F_i; F_j) \quad \text{(via the monotonicity of MI)}
\end{aligned} \tag{7}$$

C Algorithms

C.1 Partial Information Decomposition of Features

The full implementation of PIDF is presented in Algorithm 1.

Algorithm 1 Partial Information Decomposition of Features

Input: Sampled features \mathcal{F} , and target Y .

Output: $(I(F_i; Y), FWS(Y; F_i, \mathcal{F}_{\setminus F_i}), CR(Y|F_i, \mathcal{F}_{\setminus F_i}), \mathcal{R}_{\setminus F_i}) \forall F_i \in \mathcal{F}$.

```
1: for  $F_i$  in  $\mathcal{F}$  do
2:   Calculate  $I(F_i; Y)$ 
3:    $\mathcal{F}_{\setminus F_i}^{sorted} = \text{argsort}_{F_j \in \mathcal{F}_{\setminus F_i}} I(F_i; F_j)$ 
4:   Initialize  $FWR(Y|F_i, \mathcal{F}_{\setminus F_i}) = 0$  and  $\mathcal{R}_{\setminus F_i} = \emptyset$ 
5:   for  $F_j$  in  $\mathcal{F}_{\setminus F_i}^{sorted}$  do
6:     if  $I(F_i, F_j) > 0$  then
7:        $\mathcal{R}_{\setminus F_i} \cup F_j$ 
8:     end if
9:     Calculate  $\theta(Y; F_i, F_j, \mathcal{F}_{\setminus \{F_i, F_j\}}^{sorted})$ 
10:    if  $\theta(Y; F_i, F_j, \mathcal{F}_{\setminus \{F_i, F_j\}}^{sorted}) \leq 0$  then
11:       $FWR(Y|F_i, \mathcal{F}_{\setminus F_j}) = FWR(Y|F_i, \mathcal{F}_{\setminus F_j}) - \theta(Y; F_i, F_j, \mathcal{F}_{\setminus \{F_i, F_j\}})$ 
12:       $\mathcal{F}_{\setminus F_i}^{sorted} = \mathcal{F}_{\setminus \{F_i, F_j\}}^{sorted}$ 
13:    end if
14:  end for
15:   $FWS(Y; F_i, \mathcal{F}_{\setminus F_i}) = I(Y; F_i, \mathcal{F}_{\setminus F_i}) - I(\mathcal{F}_{\setminus F_i}; Y) - I(F_i; Y)$ 
16:   $\mathcal{P}^{ms} = \mathcal{F}_{\setminus F_i}^{sorted}$ 
17:  return  $I(F_i; Y), FWS(Y; F_i, \mathcal{F}_{\setminus F_i}), FWR(Y|F_i, \mathcal{F}_{\setminus F_i}), \mathcal{P}^{ms}, \mathcal{R}_{\setminus F_i}$  (Redundant FNOIs)
18: end for
```

C.2 PIDF for Feature Selection

The algorithm for feature selection based on PIDF is presented in Algorithm 2.

Algorithm 2 PIDF for Feature Selection

Input: $(FWS(Y; F_i, \mathcal{F}_{\setminus F_i}), FWR(Y|F_i, \mathcal{F}_{\setminus F_i}), I(Y; F_i), \mathcal{R}_{\setminus F_i}) \forall F_i \in \mathcal{F}$

Output: \mathcal{F}_* (a desirable feature set).

```
1: Initialize  $\mathcal{F}_* = \{\}$ .
2: for  $F_i$  in  $\mathcal{F}$  do
3:   if  $FWS(Y; F_i, \mathcal{F}_{\setminus F_i}) + I(Y; F_i) > FWR(Y|F_i, \mathcal{F}_{\setminus F_i})$  then
4:      $\mathcal{F}_* \cup F_i$ 
5:   end if
6: end for
7:  $\mathcal{F}^{sorted} = \text{argsort}_{F_j \in \mathcal{F} \setminus \mathcal{F}_*} FWS(Y; F_j, \mathcal{F}_{\setminus F_j}) + I(Y; F_j)$ 
8: for  $F_i$  in  $\mathcal{F}^{sorted}$  do
9:   if  $\mathcal{F}_* - \mathcal{R}_{\setminus F_i} = \mathcal{F}_*$  then
10:     $\mathcal{F}_* \cup F_i$ 
11:   end if
12: end for
13: return  $\mathcal{F}_*$ 
```

D Example Calculations

In this Appendix, we perform example calculations for the RVQ dataset. We first re-introduce the form of the data, before then explicitly calculating from lines 2-17 in Algorithm C.1 for feature F_0 . We only consider F_0 for space and clarity. We then calculate the results of Algorithm 2 in full. The

RVQ dataset is of the following form:

$$\begin{aligned}
F_0 &\sim \text{Bernoulli}(\mu = 0.5, \sigma = 0.5) \\
F_1 &\sim \text{Bernoulli}(\mu = 0.5, \sigma = 0.5) \\
F_2 &\equiv F_1 \\
Y &= F_0 + 2F_1.
\end{aligned} \tag{8}$$

D.1 Partial Information Decomposition of Features Calculation

Line 2: We begin by calculating $I(F_0; Y)$. Given that $y = f_0 + 2f_1$, where f_1 and f_2 can be either 0 or 1 (according to Equation 8), y can take the following values with equal chance $y \in \{0, 1, 2, 3\}$. It follows that $H(Y) = -\sum_{y \in A(Y)} p_Y(y) \log_e(p_Y(y)) = \sum_{y \in A(Y)} 0.25 \cdot 1.386 = 1.386$. Where $A(\cdot)$ is an operator that produces all possible realizations of a random variable. Upon obtaining the value of f_0 , we reduce y 's potential realizations by half. To explain this, let us suppose $f_0 = 0$. In this case, it must be true that $y = 0$ or 2 , whereas if $f_0 = 1$ it then must be true that $y = 1$ or 3 . Therefore, the following holds $H(Y|F_0) = -\sum_{y \in A(Y), f_0 \in A(F_0)} p_{Y, F_0}(y|f_0) \log_e(p_{Y, F_0}(y|f_0)) = \sum_{y \in A(Y), f_0 \in A(F_0)} 0.5 \cdot 0.693 = 0.693$. Given that $I(F_0; Y) = H(Y) - H(Y|F_0)$ it must be true that $I(F_0; Y) = 1.386 - 0.693 = 0.693$. This result agrees with the MI presented in Figure 2.

Lines 3-4: These lines are simple for variable F_0 as F_1 and F_2 have been defined such that they are independent random processes; therefore, $I(F_0; F_1) = I(F_0; F_2) = 0$ and the precise ordering of set $\mathcal{F}_{\setminus F_i}^{\text{sorted}}$ is unimportant. In this case, we let $\mathcal{F}_{\setminus F_i}^{\text{sorted}} = \{F_1, F_2\}$.

Lines 5-14: To begin we do not add F_1 to the set $\mathcal{R}_{\setminus F_i}$ as $I(F_0; F_1) = 0$. We now calculate $\theta(Y; F_0, F_1, \mathcal{F}_{\{F_0, F_1\}}) = (I(Y; F_0, \mathcal{F}_{\setminus F_0}) - I(Y; \mathcal{F}_{\setminus F_0})) - (I(Y; F_0, \mathcal{F}_{\{F_0, F_1\}}) - I(Y; \mathcal{F}_{\{F_0, F_1\}}))$. To begin, we calculate $I(Y; F_0, \mathcal{F}_{\setminus F_0}) = H(Y) = 1.386$, because the knowledge of variables $F_0, \mathcal{F}_{\setminus F_0}$ completely describes the target Y . Meanwhile, $I(Y; \mathcal{F}_{\setminus F_0}) = 0.693$, because without F_0 (via a calculation identical to that completed for $I(F_0; Y)$ above), we can only reduce the uncertainty of Y by half. Therefore, $(I(Y; F_0, \mathcal{F}_{\setminus F_0}) - I(Y; \mathcal{F}_{\setminus F_0})) = 0.693$. We now investigate the values of $I(Y; F_0, \mathcal{F}_{\{F_0, F_1\}})$ and $I(Y; \mathcal{F}_{\{F_0, F_1\}})$. Let us first note that $F_1 \equiv F_2$; consequently, by removing F_1 from \mathcal{F} , we do not diminish the set's ability to reduce the uncertainty of Y . It follows that, $I(Y; \mathcal{F}_{\setminus F_0}) = I(Y; \mathcal{F}_{\{F_0, F_1\}})$, and therefore $I(Y; F_0, \mathcal{F}_{\{F_0, F_1\}}) - I(Y; \mathcal{F}_{\{F_0, F_1\}}) = 0.693$, where $\theta(Y; F_0, F_1, \mathcal{F}_{\{F_0, F_1\}}) = 0$. Consequently, F_1 remains in $\mathcal{F}_{\setminus F_0}^{\text{sorted}}$ according to line 12.

We now repeat lines 4-14, but with FNOI F_2 . Again, we do not add F_2 to the set $\mathcal{R}_{\setminus F_i}$ as $I(F_0; F_2) = 0$. We now move onto lines 9-14 by calculating $\theta(Y; F_0, F_2, \mathcal{F}_{\{F_0, F_2\}}^{\text{sorted}})$. We note that $F_2 \equiv F_1$, as a result it must be true that $\theta(Y; F_0, F_2, \mathcal{F}_{\{F_0, F_2\}}) = \theta(Y; F_0, F_1, \mathcal{F}_{\{F_0, F_1\}}) = 0$. Therefore, for feature F_0 , we return $I(F_0; Y) = 0.693, FWS(Y; F_0, \mathcal{F}_{\setminus F_0}) = 0, FWR(Y|F_0, \mathcal{F}_{\setminus F_0}) = 0, \mathcal{R}_{\setminus F_i} = \{\}$.

Above we have calculated from lines 2-17 in Algorithm C.1 for variable F_0 in the RVQ dataset. By applying the same procedure, one can obtain the following values for F_1 : $I(F_1; Y) = 0.693, FWS(Y; F_1, \mathcal{F}_{\setminus F_1}) = 0, FWR(Y|F_1, \mathcal{F}_{\setminus F_1}) = 0.693$, with $\mathcal{R}_{\setminus F_i} = \{F_2\}$. Similarly, for F_2 : $I(F_2; Y) = 0.693, FWS(Y; F_2, \mathcal{F}_{\setminus F_2}) = 0, FWR(Y|F_2, \mathcal{F}_{\setminus F_2}) = 0.693$, and again $\mathcal{R}_{\setminus F_i} = \{F_1\}$.

D.2 Feature Selection Calculation

We will now utilize the results obtained from the PIDF calculations in the previous section to select features. This will be done by explicitly carrying out the calculations as per Algorithm 2.

Lines 1-6: From the results generated in the last section, it is clear that $I(F_0; Y) + FWS(Y; F_0, \mathcal{F}_{\setminus F_0}) - FWR(Y|F_0, \mathcal{F}_{\setminus F_0}) = 0.693$, and therefore F_0 is included in the set of selected features ($\mathcal{F}_* = \{F_0\}$). However, this is not the case for F_1 and F_2 . For F_1 we calculate $I(F_1; Y) + FWS(Y; F_1, \mathcal{F}_{\setminus F_1}) - FWR(Y|F_1, \mathcal{F}_{\setminus F_1}) = 0.693 + 0 - 0.693 = 0$. Similarly, for F_2 we get $I(F_2; Y) + FWS(Y; F_2, \mathcal{F}_{\setminus F_2}) - FWR(Y|F_2, \mathcal{F}_{\setminus F_2}) = 0.693 + 0 - 0.693 = 0$. Consequently, neither F_1 or F_2 are added to our set of selected features at this stage.

Lines 7-12: We begin by ordering the non-selected features by their total information $I(F_i; Y) + FWS(Y; F_i, \mathcal{F})$ (line 7). However, in this case, we have $I(F_1; Y) + FWS(Y; F_1, \mathcal{F}) = 0.693$

and $I(F_2; Y) + FWS(Y; F_2, \mathcal{F}) = 0.693$; therefore, the order is not meaningful. To complete the calculation, we let $\mathcal{F}^{sorted} = \{F_1, F_2\}$, and apply line 9. Currently, we have $\mathcal{F}_* = \{F_0\}$ and $\mathcal{R}_{\setminus F_1} = \{F_2\}$, therefore $\mathcal{F}_* - \mathcal{R}_{\setminus F_1} = \mathcal{F}_*$ and F_1 is added to the set \mathcal{F}_* , such that $\mathcal{F}_* = \{F_1, F_2\}$. Now repeating this step for F_2 , we have $\mathcal{F}_* = \{F_0, F_1\}$ and $\mathcal{R}_{\setminus F_2} = \{F_1\}$, it is trivial to see that $\mathcal{F}_* - \mathcal{R}_{\setminus F_2} = \{F_0\} \neq \mathcal{F}_*$. As a result F_2 is not added to our final set of selected features, and our final result is $\mathcal{F}_* = \{F_0, F_1\}$.

E Hyperparameter Selection Discussion

For both the feature selection and feature interpretation experiments we used a simple grid search when deciding hyperparameters. PIDF, TERC and the method introduced by Wollstadt et al. [2023] all rely on the calculation of MI. As discussed in Section A.1, we estimate MI across all methods using the 5 repetitions of the techniques described by Belghazi et al. [2018]. For clarity regarding hyperparameters, we present the details of this technique in Algorithm 3.

Algorithm 4 MINE Belghazi et al. [2018].

Input: Training dataset $(f^1, y^1, f^2, y^2 \dots f^T, y^T)$

Output: $I(Y; F)$

- 1: Initialize weights θ .
 - 2: **for** 1 to N **do**
 - 3: Draw mini batch samples of length b from the joint distribution of the actions and the state with all possible variables included $p_{Y,F} \sim ((y^1, f^1), \dots, (y^b, f^b))$, and repeat for the marginal distribution $p_{Y \otimes F} \sim ((y^1, f^r), \dots, (y^b, f^r))$ (where the superscript r indicates random sampling).
 - 4: $I(Y; F) = \frac{1}{b} \sum^b F_\theta((y^1, f^1), \dots, (y^b, f^b)) - \frac{1}{b} \sum^b \log e^{F_\theta((y^1, f^r), \dots, (y^b, f^r))}$
 - 5: $\theta \leftarrow \tilde{\nabla}_\theta I(Y; F)$
 - 6: **end for**
 - 7: **return** $I(Y; F)$
-

E.1 Explaining Data Hyperparameters

For PIDF we selected $b = 1000$, $N = 20,000$ as defined in Algorithm 4. Meanwhile, the learning rate of the network in use was $\alpha = 0.0001$ with an adam optimizer. Each network had one hidden layer consisting of 50 neurons. For UMF1 and MCI, 100 trees were selected as optimal. Otherwise, hyperparameters were as described in Janssen et al. [2023] and Catav et al. [2021] respectively. For PI, we also selected 100 random trees.

E.2 Feature Selection Hyperparameters

For PIDF, TERC and the Wollstadt method we again selected $b = 1000$, $N = 20,000$ as defined in Algorithm 4. Meanwhile, the learning rate of the network in use was $\alpha = 0.0001$. For PI, we again selected 100 random trees.

F Example of How to Interpret the Results of PIDF

In this section, we discuss an example of how to interpret the results of PIDF, we refer to Figure 3. In this illustration, the top row represents the results of PIDF. We guide the reader through the Wollstadt toy example dataset, as it is known to be characterized by both redundant and synergistic relationships (as shown in the graph titled WT)[Wollstadt et al., 2023]. Firstly, we investigate the bars associated with F_0 ; in this case, F_0 is our FOI, while the remaining features make up the FNOI. We observe that F_0 provides significant information regarding the target. However, it is also clear that the majority of this information is redundant with respect to the FNOI F_1 . We know the feature is redundant with respect to F_1 due to the 1 in the purple bar (i.e., the numbers in the bars represent the subscripts of the involved FNOI). If we now investigate the relationships associated with the feature F_1 (making this the FOI), we observe that this feature also provides significant information; however,

it is entirely redundant with respect to F_0 . Finally, investigating F_2 , we see this final feature combines with F_0 to provide some non-redundant synergistic information. We can tell this combination occurs with F_0 due to the green 0 above the bar. Consequently, using Figure 2 we have now understood the following relationships in the data:

1. F_0 provides significant information; although, some of it is redundant with respect to F_1 .
2. F_1 provides significant information; however, *all* of it is redundant with respect to F_0 (this indicates that F_0 contains all the information in F_1 and some).
3. F_2 combines synergistically with F_0 to provide some non-redundant information [Wollstadt et al., 2023].

G Mathematical Description of Synthetic Datasets

Redundant variables question dataset (RVQ). This dataset is comprised of three stochastic binary arrays, F_0, F_1, F_2 of length 1000, two of which are fully redundant with respect to one another. More formally, we have:

$$\begin{aligned}
 F_0 &\sim \text{Bernoulli}(\mu = 0.5, \sigma = 0.5) \\
 F_1 &\sim \text{Bernoulli}(\mu = 0.5, \sigma = 0.5) \\
 F_2 &\equiv F_1 \\
 Y &= F_0 + 2 * F_1.
 \end{aligned} \tag{9}$$

Synergistic variables question dataset (SVQ). The features are two stochastic binary arrays, F_0, F_1 of length 1000, where $Y = XOR(F_0, F_1)$ and $F_0 \neq F_1$. As explained in Section A.2, F_0 and F_1 have been defined such that they combine to provide synergistic information about the target. More formally:

$$\begin{aligned}
 F_0 &\sim \text{Bernoulli}(\mu = 0.5, \sigma = 0.5) \\
 F_1 &\sim \text{Bernoulli}(\mu = 0.5, \sigma = 0.5) \\
 Y &= XOR(F_0, F_1).
 \end{aligned} \tag{10}$$

Multiple subsets question dataset (MSQ). The features are three stochastic binary arrays, F_0, F_1, F_2 of length 1000; where, $Y = F_0 = F_1 + F_2$. This can be re-written:

$$\begin{aligned}
 F_1 &\sim \text{Bernoulli}(\mu = 0.5, \sigma = 0.5) \\
 F_2 &\sim \text{Bernoulli}(\mu = 0.5, \sigma = 0.5) \\
 Y &= F_0 = F_1 + F_2.
 \end{aligned} \tag{11}$$

Wollstadt toy dataset (WT). The Wollstadt toy example is characterized by three features, formed by combining normal distributions:

$$\begin{aligned}
 \epsilon_1 &\sim \mathcal{N}(\mu = 0, \sigma = 1) \\
 \epsilon_2 &\sim \mathcal{N}(\mu = 0, \sigma = 1) \\
 \epsilon_3 &\sim \mathcal{N}(\mu = 0, \sigma = 1) \\
 F_0 &= \epsilon_1 + 0.1F_2 \\
 F_1 &= 0.8\epsilon_1 + 0.2\epsilon_2 + 0.01 * F_2 \\
 F_2 &\sim \mathcal{N}(\mu = 0, \sigma = 1) \\
 Y &= \sin(\epsilon_1) + 0.1\epsilon_3.
 \end{aligned} \tag{12}$$

TERC-1. This dataset, introduced by Westphal et al. [2024], contains six features, with the following characteristics:

$$\begin{aligned}
F_0 &\sim \text{Bernoulli}(\mu = 0.5, \sigma = 0.5) \\
F_1 &\sim \text{Bernoulli}(\mu = 0.5, \sigma = 0.5) \\
F_2 &\sim \text{Bernoulli}(\mu = 0.5, \sigma = 0.5) \\
F_3 &\equiv F_0 \\
F_4 &\equiv F_0 \\
F_5 &\equiv F_0 \\
Y &= \begin{cases} 0, & \text{if } f_1 = f_2 = f_3 \\ 1, & \text{otherwise} \end{cases}
\end{aligned} \tag{13}$$

TERC-2. This dataset, introduced by Westphal et al. [2024], contains six features, with the following characteristics:

$$\begin{aligned}
F_0 &\sim \mathcal{N}(\mu = 0, \sigma = 1) \\
F_1 &\sim \text{Bernoulli}(\mu = 0.5, \sigma = 0.5) \\
F_2 &\sim \text{Bernoulli}(\mu = 0.5, \sigma = 0.5) \\
F_3 &\equiv F_0 \\
F_4 &\equiv F_1 \\
F_5 &\equiv F_2 \\
Y &= \begin{cases} 0, & \text{if } f_1 = f_2 = f_3 \\ 1, & \text{otherwise} \end{cases}
\end{aligned} \tag{14}$$

UMFI blood relation dataset (UBR). Janssen et al. [2023] used the UBR dataset to demonstrate that their method had favorable properties in detecting blood relationships in causal graphs. This dataset is characterized by four features with the following characteristics.

$$\begin{aligned}
\epsilon_1 &\sim \mathcal{U}(\mu = -1, \sigma = 1) \\
\epsilon_2 &\sim \mathcal{U}(\mu = -0.5, \sigma = 0.5) \\
\epsilon_3 &\sim \text{Exp}(1) \\
\epsilon_4 &\sim \mathcal{N}(\mu = 0, \sigma = 1) \\
F_0 &\sim \mathcal{N}(\mu = 0, \sigma = 1) \\
F_1 &= 3F_0 + \epsilon_1 \\
F_2 &= \epsilon_4 + F_0 \\
F_3 &= Y + \epsilon_3 \\
Y &= \epsilon_4 + \epsilon_2.
\end{aligned} \tag{15}$$

Synthetic genes dataset (SG). Our final synthetic dataset was developed in Anastassiou [2007] to demonstrate the types of relationships that could be present in genetic interactions. Formally Y is:

$$Y \sim \text{Bernoulli}(\mu = 0.5, \sigma = 0.5), \tag{16}$$

where $y = 1$ indicates cancer. The features meanwhile can be explained via the following bullet points:

- In healthy samples, the probability that both $f_1 = f_2 = 1$ is 95%, whereas the remaining three joint states (00, 01 and 10) are equally likely. Meanwhile, in cancerous samples, the probability that both $f_1 = f_2 = 1$ is 5%, whereas the remaining three joint states (00, 01 and 10) remain equally likely.
- In healthy samples, if $y = 0$, then $F_3 \sim \text{Bernoulli}(\mu = 0.2, \sigma = 0.5)$. Meanwhile, in cancerous samples, we have $F_3 \sim \text{Bernoulli}(\mu = 0.8, \sigma = 0.5)$.

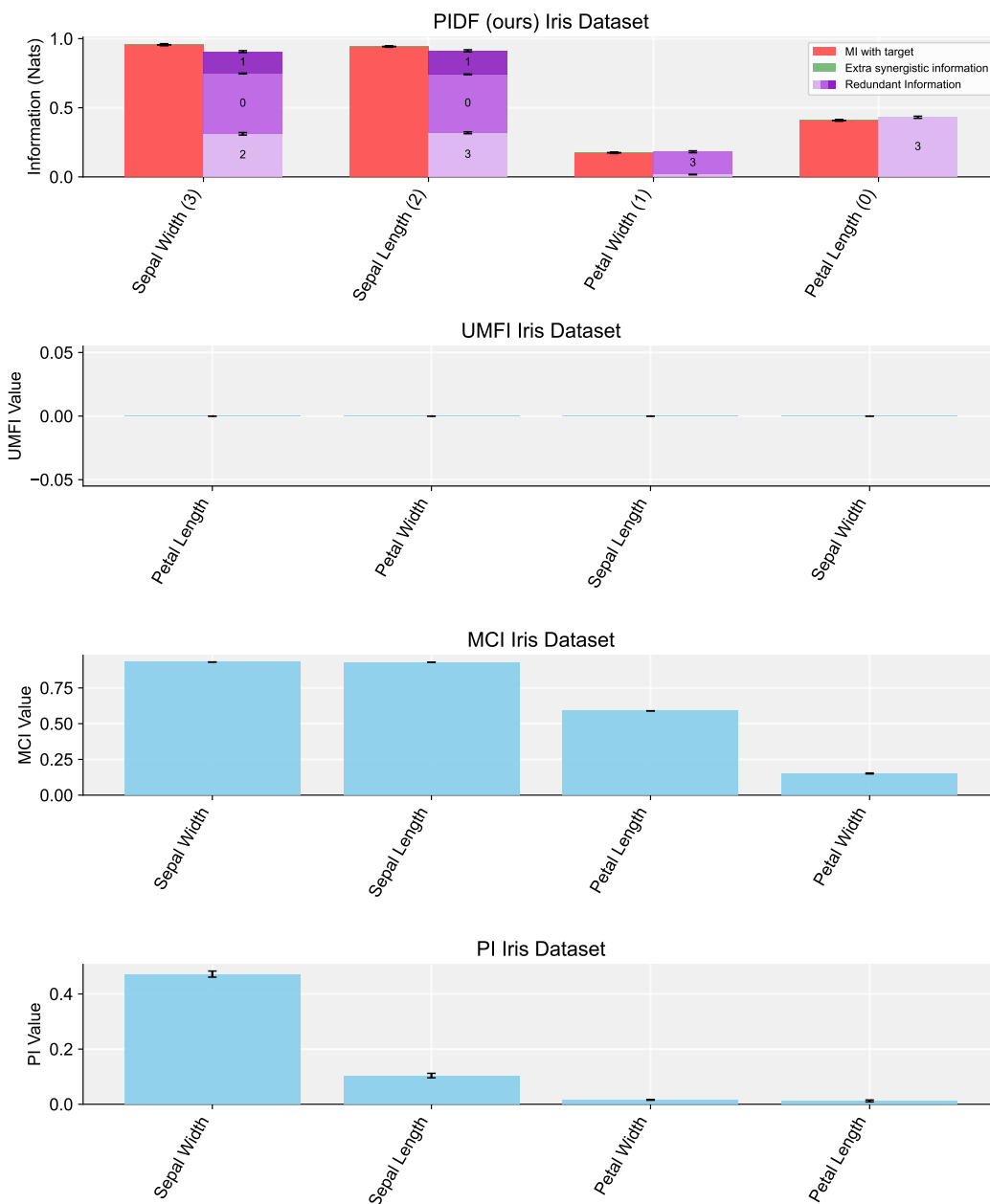


Figure 7: Comparison of feature importance methods using the classic Iris dataset.

H Sampling Method for Neural Culture Data

We now provide more details regarding the firing neurons dataset, including the methods we used to sample from it. This dataset was introduced in Wagenaar et al. [2006] and is publicly accessible online⁴. These datasets comprise multiunit spiking activities recorded from each of the 60 electrodes in the multi-electrode array used to study the activations of dissociated neural cells. Specifically, the data from neural culture 2-2 were utilized. Comprehensive details regarding the cultivation and maintenance of these cultures are documented in Wagenaar et al. [2006]. The analysis focused on recordings from eight developmental stages of the culture, measured in days in vitro (DIV):

⁴<https://potterlab.gatech.edu/potter-lab-data-code-and-designs/>

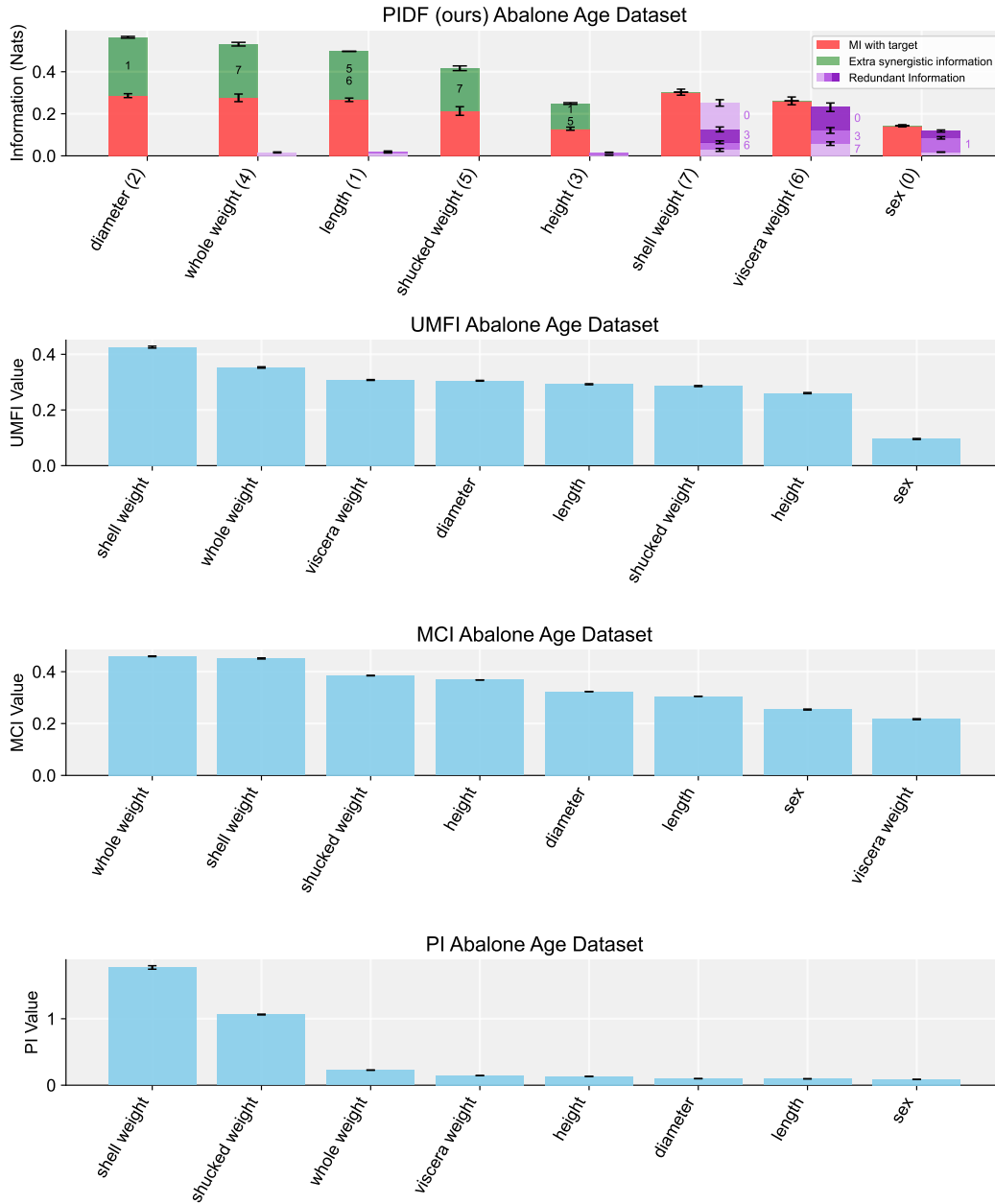


Figure 8: Comparison of feature importance methods using the classic Abalone dataset.

4, 7, 12, 16, 20, 25, 31, and 33. The recording from DIV 16 lasted for 60 minutes, while the recordings from the other days each lasted for 45 minutes. For the purposes of this analysis, the data were segmented into bins of $16 \mu s$. The probability distributions required for calculating the three information-theoretic quantities of interest were generated by analyzing the spike trains from groups of ten distinct electrodes. Within each group, one electrode was randomly designated as the Y variable, and the remainder as the features. For every time step in the spike trains, the states (spiking or not) of the feature electrodes at time t and the Y electrode at time $t + 1$ were noted. This tabular data could then act as input to Algorithms 4 and C.1. This procedure was replicated for each set of non-identical electrodes, ensuring that groups with interchanged features were only considered once to prevent duplication. A full discussion of this dataset can be found in Timme and Lapish [2018].

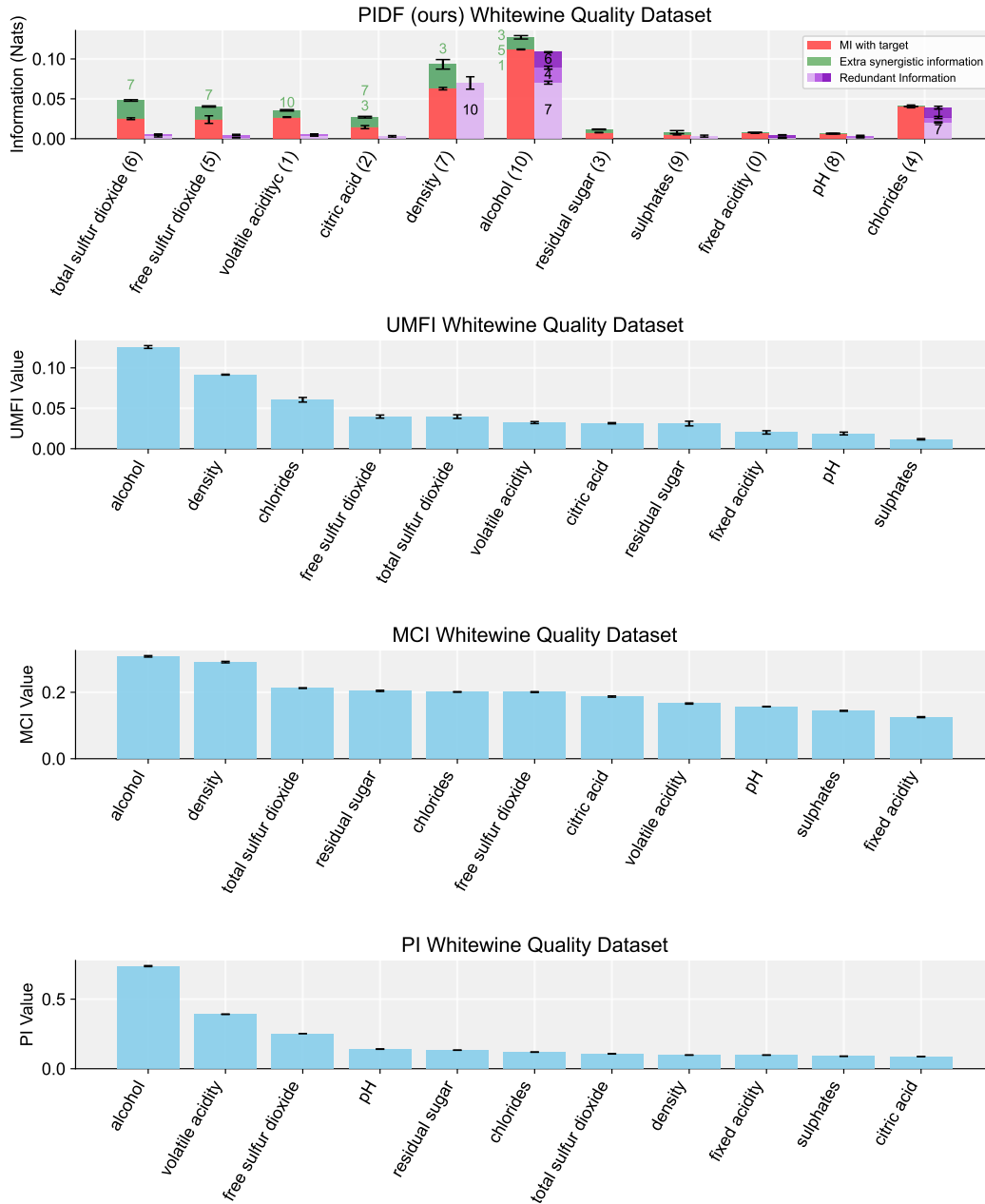


Figure 9: Comparison of feature importance methods using the classic whitewine quality dataset.

I Further Experiments on Classic Machine Learning Datasets

I.1 Iris Dataset

In this section, we apply PIDF to the Iris dataset. One of the earliest and best-adopted datasets in ML, Iris was used to predict flower type given the petal length and width and sepal length and width.

In Figure 7, we observe that, unsurprisingly, there is a large amount of redundancy between the features in the Iris dataset. UMFI's pre-processing step, which removes redundancies between pairwise features, is unable to resolve the more complex redundancies we see Figure 7; hence, the assignment of feature importance scores of 0. Meanwhile, PIDF is the only method able to reveal the

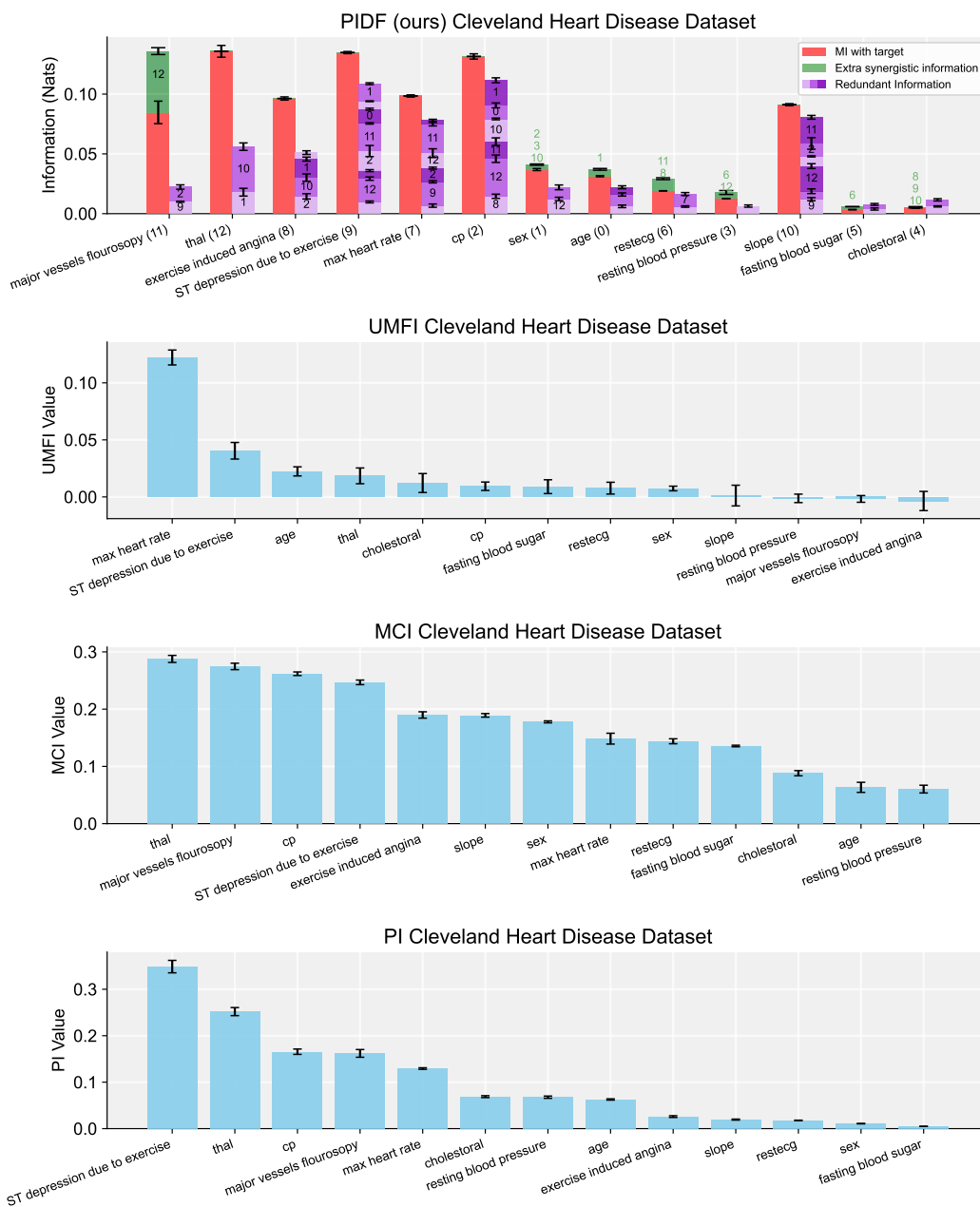


Figure 10: Cleveland heart disease prediction experiments.

complex set of redundancies, showing that sepal width and sepal length are both well correlated with the target. But the sepal width also provides redundant information with respect to the petal length and width, making this the most informative feature, as revealed using PI.

I.2 Abalone Dataset

In this section, we apply PIDF to the Abalone dataset, which comprised information about the size and weight of an Abalone, and is used to predict its age.

In Figure 8, it is possible to observe that in this everyday dataset we see synergistic interactions occurring. The whole weight and shucked weight combine synergistically with the shell weight.



Figure 11: Feature duplication experiments. We apply PIDF to a modified version of the California housing, Abalone, and Whitewine datasets. These modified datasets are obtained by adding a duplicate feature to the original ones. The duplicate features we used in our experiments are longitude, diameter and density, respectively.

Intuitively, this makes sense as finer grained detail about the weights of individual components of the animal may lead to greater knowledge of the animals age. Meanwhile, we observe that the viscera weight and shell weight are redundant with respect to one another, while this is not the case with whole and shucked weights.

I.3 Whitewine Dataset

In this section, we apply PIDF to a classic ML dataset, which uses the chemical properties of wine to predict its quality.

In Figure 9, we observe that the alcohol levels and density provide redundant information with respect to each other. This redundancy can be attributed to the fact that, apart from alcohol, wine primarily consists of water-based solubles. Consequently, the density of the wine is a function of the

alcohol-water ratios. Interestingly, we see that the free and total sulfur dioxide features are not highly redundant with respect to one another. This is because, during the wine-making process, free sulfur dioxide is added for anti-microbial effects. Meanwhile, the bound sulfur dioxide is more dependent on the grape used.

I.4 Cleveland Heart Disease Dataset

In this section, we apply PIDF to a classic ML dataset, which uses medical data to predict cases of heart disease in Cleveland, Ohio.

In Figure 10, we observe that thalassemia intermedia and the number of major articles with blockages as detected by fluoroscopy combine synergistically to predict heart disease.

J Feature Duplication Experiments

In the main body of the paper, we demonstrated that our method could be used to successfully detect redundancies in synthetic data. Extending this validation, inspired by experiments in Catav et al. [2021], we now demonstrate our method’s ability to illuminate known redundancies in real-world datasets. This is achieved by duplicating features within the, widely recognized, California housing, Abalone, and Whitewine ML datasets. Subsequently, we provide evidence demonstrating the successful detection of these introduced redundancies by our methodology. These duplicated features will simply be added to the original datasets.

In Figure 11, we showcase the outcomes from our experiments on duplicated features. The findings demonstrate that FWS and MI of the duplicated features mirror that of their non-duplicated counterparts. However, the information provided by these features is now redundant.

K Computational Requirements

In its current form, the execution of PIDF requires more computational resources than its other counterparts for feature interpretability Catav et al. [2021], Janssen et al. [2023]. For example, executing the results for the TERC-1 and TERC-2 datasets, which contained six features each with 1000 instances took 45 minutes on a P100 NVIDIA GPU cluster. At the same time, it is worth noting that the methods are not directly comparable, given the algorithmic steps that are necessary for analyzing interactions between variables. The temporal complexity of the method scales as a function k^2 , where k is the number of features. Consequently, in its current format PIDF is not appropriate for very-large feature spaces. As part of our research agenda, we plan to investigate the following two potential solutions for speeding-up the implementation of PIDF:

1. As discussed in the conclusion, a hierarchical approach can be adopted. Rather than removing individual redundant features, as per line 12 of Algorithm C.1, many can be checked and removed at once.
2. Another way in which it is possible to scale the PIDF implementation is by enhancing the efficiency of the MI estimation. Currently, we use MINE [Belghazi et al., 2018], as the results are in Nats, which are easily interpretable. However, if one wishes just to compare the relative values of PIDF, without the need for values with units, more efficient methods can be used. In particular, we will make available a version of PIDF implemented using the method developed in Covert et al. [2020].